ASSESSMENT ON EFFECT OF GEOMETRY DEFECT FOR STEEL PIPE

RABBIATUL ADDAWIYYAH BT AHMAD BUSTAMAN

Report submitted in partial fulfillment of the requirements for the award of the degree of Bachelor of Mechanical Engineering

Faculty of Mechanical Engineering
UNIVERSITI MALAYSIA PAHANG

JUNE 2013

EXAMINER'S DECLARATION

UNIVERSITI MALAYSIA PAHANG

FACULTY OF MECHANICAL ENGINEERING

I certify that the project entitled "*Assessment on Effect of Geometry Defect for Steel Pipe*" is written by *Rabbiatul Addawiyyah Bt Ahmad Bustaman.* I have examined the final copy of this project and in my opinion, it is fully adequate in terms of language standard and report formatting requirement for the award of the degree of Bachelor Engineering. I herewith recommend that it be accepted in partial fulfillment of the requirements for the degree of Bachelor Mechanical Engineering.

Dr. YULI PANCA ASMARA

Examiner Signature

SUPERVISOR'S DECLARATION

I have examined the final copy of this report and in my opinion, it is satisfactory in terms of language standard, and report formatting requirement for the award of the degree of Bachelor Mechanical Engineering.

Signature:

Name of Supervisor: PN. NORHAIDA BT AB. RAZAK

Position:

Date: 26 June 2013

STUDENT’S DECLARATION

I declare that this project titled “ASSESSMENT ON EFFECT OF GEOMETRY DEFECT FOR STEEL PIPE” is my result of my own research except as stated in the references. This report has not been accepted for any degree and is not concurrently submitted for award of another degree.

Signature:

Name: RABBIATUL ADDAWIYYAH BT AHMAD BUSTAMAN

Id. Number: MA09113

Date: 26 JUNE 2013

Dedicated, truthfully for supports,
encouragements and always be there during hard times,
to my beloved parent, siblings and friends.

ACKNOWLEDGEMENT

First of all, I would like to express my highest gratitude to Allah the Almighty for blessing me in finishing this project. Besides, I would like to take this opportunity to express my sincere gratitude and appreciation especially to my supervisor, Mrs. Norhaida Binti Abd Razak for her constant guidance, consideration and constructive idea in leading me to accomplish this project. Thanks a lot for giving me a professional training, advice and suggestion to bring this thesis to its final form. Without her support and interest, this thesis would not have been the same as presented here. I am very grateful for her patience and constructive comments that enriched this research project.

Besides that, I would like to acknowledge with much appreciation the crucial role of the staff in Analysis Room Faculty of Mechanical, for their valuable comments, sharing their time and knowledge on this research project during the project was carried out and giving a permission to use all the necessary tools in the laboratory. They have contributed towards my understanding and thoughts.

Last but not least, an expression of thanks is extended to everyone who has offered their help and support especially to my family and friends. All of their helps are very significant to the success of this project. I cannot find the appropriate words that could properly describe my appreciation for their devotion, support and faith in my ability to attain my goal.

ABSTRACT

The aim of this research is to study the effect of geometry defects for steel pipe subjected to stress-based criteria. The objectives for this project are to simulate the effect of corrosion geometry on steel pipeline with variable defect depth and to determine the maximum pressure on different defect geometry. This study focused on effect of width and depth defect for rectangular and groove defect. The scope of research consists of material made of API 5L grade B which involve of elastic and plastic deformation. The MSC Marc 2008r1 is used to simulate 2-D corrosion defect of pipeline which involved groove defect and rectangular defect with variables in depth and width defect. There are three different widths (0.2mm, 0.5mm and 1mm) and depths (20%, 50% and 75% from the wall thickness) are selected to be analysed. The simulation involved about 18 designs of defects. Meanwhile, half of the pipe model with the outer diameter of 60.5mm and wall thickness 4mm were simulated to analyse the defect condition. The FEA result will be compared in terms of depth defect and length of width. Besides, it also will be compared with the industry codes such as ASME B31G, Modified ASME and DNV-RP-F101. Based on analysis, the width of defect does not affect much upon the burst pressure. However, depth of corrosion defect plays an important role for the pipeline to be failed in operation. The deep defect is easily reach burst pressure compare to the shallow defect and moderately defect. On the top of that, the FEA result for burst pressure is much higher rather than industry codes. From the analysis done, the groove defect and rectangular defect tends to failed at almost the same burst pressure even the width is different. In a nutshell, the depth of corrosion defect plays an important role for burst pressure rather than width. Moreover, the different type of defect does not give huge impact on the burst pressure.

ABSTRAK

Tujuan kajian ini adalah untuk mengkaji kesan kecacatan geometri bagipaip keluli tertakluk kepada kriteria berasaskan tekanan. Objektif projek ini adalah untuk meniru kesan geometri karat pada paip keluli dengan kedalaman kecacatan berubah dan untuk menentukan tekanan maksimum kepada geometri kecacatan yang berbeza. Kajian ini memberi tumpuan kepada kesan lebar dan kedalaman kecacatan kecacatan segi empat tepat dan alur. Skop penyelidikan terdiri daripada bahan yang diperbuat daripada API 5L gred B yang melibatkan ubah bentuk anjal dan plastik. MSC Marc 2008r1 digunakan untuk mensimulasikan 2-D hakisan kecacatan saluran paip yang melibatkan kecacatan dan kecacatan alur segi empat tepat dengan pembolehubah secara mendalam dan kecacatan lebar. Terdapat tiga lebar yang berbeza (0.2mm, 0.5mm dan 1mm) dan kedalaman (20%, 50% dan 75% daripada ketebalan dinding) yang dipilih untuk dianalisis. Simulasi ini melibatkan kira-kira 18 reka bentuk kecacatan. Sementara itu, separuh daripada model paip dengan diameter luar 60.5mm dan dinding tebal 4mm adalah simulasi untuk menganalisis keadaan kecacatan itu. Hasil FEA akan dibandingkan dari segi kecacatan mendalam dan panjang lebar. Selain itu, ia juga akan dibandingkan dengan kod industri seperti ASME B31G, Modified ASME dan DNV-RP-F101. Berdasarkan analisis, lebar kecacatan tidak menjejaskan banyak kepada tekanan pecah. Walau bagaimanapun, kedalaman kecacatan karat memainkan peranan yang penting untuk saluran paip yang akan gagal dalam operasi. Kecacatan dalam mudah mencapai tekanan pecah berbanding dengan kecacatan itu cetek dan kecacatan sederhana. Di samping itu, keputusan FEA untuk tekanan pecah adalah lebih tinggi daripada kod industri. Daripada analisis yang dilakukan, kecacatan alur dan kecacatan segiempat cenderung untuk gagal di hampir tekanan pecah sama walaupun lebar adalah berbeza. Secara ringkas, kedalaman kecacatan karat memainkan peranan yang penting untuk tekanan pecah bukannya lebar. Manakala, jenis kecacatan yang berbeza tidak memberi impak yang besar terhadap tekanan pecah.

TABLE OF CONTENTS

LIST OF TABLES

LIST OF FIGURES

LIST OF SYMBOLS

D	Outside diameter
D_i	Inside diameter
d	Defect depth
t	Wall thickness
L	Longitudinal corrosion defect length
P_b or P_f	Failure pressure
M	Bulging factor
R	Average pipe radius
σ_y	Yield stress
σ_f	Flow stress
σ_U	Ultimate tensile stress
Q	Corrector factor
Q_I	Oxidation charge during the fast steady oxidation period
Q_{II}	Oxidation charge during the protective oxide film recovery period
Q_{III}	Oxidation charge during the steady passive state

LIST OF ABBREVIATONS

2D	Two Dimensions
ASME	American Society for Mechanical Engineer
API	American Petroleum Institute
DNV	Det Norske Veritas
FEA	Finite Element Analysis
SMYS	Specified minimum yield strength of pipe steel
SMTS	Specified minimum tensile strength of pipe steel

CHAPTER 1

INTRODUCTION

1.1 INTRODUCTION

This chapter will briefly explain about the introduction of this project task. The introduction is general information regarding the topic that will be discussed with this project. This topic will consist of background of proposed study, problem statement, objectives, scope of research and significant research. That information is important before further discuss to the analysis and study case later.

1.2 BACKGROUND OF PROPOSED STUDY

Pipelines have been used as one of the most economical, highest capacity and safety ways in transmitting oil and gas. However, a number of pipelines are still under construction all over the world which dramatically rising number of operating pipelines (Choi *et. al.*, 2003). The material properties of the pipelines yet been improved in terms of corrosion and yield strength of steel, to reduce failure during operation and decreases cost for maintenance (Amirat *et. al.*, 2006). However, the increasing of pipeline aging in operation may increase accident, causes by internal and external corrosion defects (Teixeira *et al.*, 2008). Major failures of pipeline causes by external defects are corrosion defects, gouges, foreign object scratches and pipe erection activities (Abid *et al.*, 2006). Some sections of high pressure pipeline may experience corrosion after long service histories (Ma *et al*., 2013).

The corrosion failure on the pipelines caused wall thinning on the inner and outer surface; generate stress concentration in the pipe wall. Moreover, defects due to localized corrosion have high failure risk to the pressurized pipelines (Xu and Cheng, 2012). The dimensions such as length, width and depth of corrosion defects influence the stress concentration to different extent (Length of the defect refer to the longitudinal, the width of the defect refers to the longitudinal, the width of the defect refers to the circumferential direction of the pipelines.) (Fekete and Varga, 2012).

Pipelines provide safe high-capacity transportation of natural gas and other products. Defects on the pipeline will take the operation under risk. Prediction of the burst pressure is relevance to pipeline industry (Zhou and Huang, 2012). Burst pressure is defines as limit load or failure pressure of pipe at plastic collapse, representing the maximum load bearing capacity of the pipe (Ma *et al.*, 2013).

1.3 PROBLEM STATEMENT

Recently, there are highly demand of natural gas all over the world, has simulated development of a complex pipeline network necessary to carry natural gas from extraction fields to storage sites. Accurate prediction of residual strength corroded piping system remains essential in fitness for service analyses of oil and gas transmission pipelines. To assess the integrity of corroded piping system, conventional procedure is used with axial defects generally employ simplified failure upon a plastic collapse failure mechanism incorporating the tensile properties of the pipe material (Mario *et. al*., 2009).

Failure may provide significant scatter in predictions, which lead to unnecessary repair or replacement of in service pipelines and about to increase the cost of maintenances. Central focus is to gain additional insight into effects of defect geometry and material properties in attainment local limit load for support development of stress-based burst strength criteria (*Mario et. al.*, 2009).

1.4 OBJECTIVES

For this project, main objective are listed:

a) To simulate the effect corrosion geometry on steel pipeline with variable defect depth and width.
b) To analyse the effect of maximum pressure on different defect geometry.

1.5 SCOPE OF RESEARCH

This study was focused on the effect of defect width and defect depth. The step consists of:

a) Used material made of API 5L, material grade B (API 5L L245).
b) To simulate the defect by using Software MSC Marc 2008 r1.
c) This simulation consists of elastic and plastic deformation.
d) To simulate 2D defect

1.6 SIGNIFICANT OF RESEARCH

This research is focusing on the assessment on effect of geometry defect for steel pipeline. The scope of this research is as below:

a) To simulate defect using finite element analysis.
b) To studies of different depth of defect and defect of geometry.

CHAPTER 2

LITERATURE REVIEW

2.1 INTRODUCTION

This chapter will briefly explain about the material used, defect over the pipeline and method in industries by solving the corrosion problem. The sources are taking from the journals, and articles and books. The literature review is helping in order to provide important information regarding previous research which related to this project. Those information are important to know before can proceed further to analysis and study later.

2.2 INTRODUCTION OF PIPELINE

Pipelines are built for transporting liquids and gases such as oil and natural gas, which commonly used in offshore and onshore industries. However, pipelines have its own time limitation before its failure in operation which being affected because of increasing of aging infrastructure. The failure of the pipelines during operation may expose accidences to be occurred. Most of the accidents occurred in natural gases and liquids pipelines are internal and external defects (Teixeira *et.al.,* 2008). The geometry defect occurred from the corrosion and material properties will affect the limit load of the pipelines before it burst. In order to reduce any potential due to undue accident caused by a lack of unawareness of integrity of the line, regular inspection of pipelines is needed.

2.3 Material in pipeline

Pipelines material is chosen by considering about their mechanical properties. High grade steel pipe is used in transporting liquid and gases over long distances in onshore and offshore (Tanguy *et.al*., 2008). There are many types of grade steel which used in pipelines such as X52, X60, X65, X70, X100, API X52 and so on. Every pipeline have its own grade, those grades will distinguish the strength of the pipe. For example the differences of chemical properties of X52 steel and X60 steel based on the table 1 below.

Table 2.1: Chemical Composition of the steels (mass %) (Tanguy *et. al*, 2008)

Steel	C	Mn	Si	P	S	Cr	Ni	V	Nb	Ti
X52	0.09	0.92	0.28	0.007	0.010	0.02	0.01	0.004	0.03	0.01
X60	0.21	1.52	0.19	0.012	0.003	0.16	0.15	0.05	0.03	0.01
X42	0.18	0.84	0.22	0.013	0.004	0.07	0.02	-	-	-

During 1950-1960, API X52 was the common material to build gas pipelines for transmission of oil and gas. The composition of the chemical composition for API X52 is shown in Table 2.2.

Table 2.2: Chemical composition of API X52 (weight %) (Adib *et.al*., 2006)

Steel	C	Mn	Si	Cr	Ni	Mo	S	Cu	Ti	Nb	Al
API X52	0.22	1.22	0.24	0.16	0.14	0.06	0.036	0.19	0.04	<0.05	0.032

Table 2.3: Chemical composition of X-65 pipeline steel (wt%). (Cheng, 2007)

Steel	C	Mn	P	Si	Cr	Ni	Cu	Nb	Al
API X65	0.11	1.50	0.013	0.26	0.006	<0.02	0.04	0.04	0.05

2.4 Type of defect in pipelines

Transmission pipelines of oil and gases have a high safety record due to a combination of good materials, design and operating practices. Major failure causing defects in gas pipeline is an external defect such as corrosion defects, gouges, foreign object scratches and pipeline erection activities (Adib *et.al*., 2007). However, external interference (known as mechanical damage) and corrosion on the surface of the pipeline causes damage and failure of the transmission pipelines. Moreover, corrosion and ground movement are two important causes resulting failure to the pipelines. Corrosion can cause defects to the pipelines due to reduction of pipeline structural integrity which increase the risk of failure. Movement of ground will produce longitudinal loads on the pipe, creating stress strain to threaten the safety of pipeline (Xu and Cheng, 2012). Dents and gouges known as mechanical damages affected on pipelines which cause adverse effects on pipeline integrity. Meanwhile, it causes local stress and also strains concentration to the pipelines (Jacob *et.al*., 2010).

2.4.1 Corrosion

Each year millions of dollars are lost because of corrosion occurred. It causes metal loss of the surface of the pipeline. The one of major reasons causing pipeline defects is corrosion. Mostly, this loss is due to corrosion of iron and steel even though there are many other metals may corrode as well (e.g. ceramics or polymers). Corrosion happens due to the electrochemical process. Usually, corrosion appears as either corrosion or localized (pitting) corrosion. There are a few types of corrosion normally occurred in pipeline, including galvanic corrosion, microbiologically induce corrosion, AC corrosion, differing soils, differential aeration and cracking (Cosham *et.al.*, 2007). Generally failures occur due to corrosion are associated with sweet (CO2) and sour (H2S) producing fluids. Corrosion defects on pipeline have a complex geometry, it been assumed as having semi-elliptical shape in some well-known codes. The radial corrosion on normal probability paper is illustrated as in Figure 2.1.

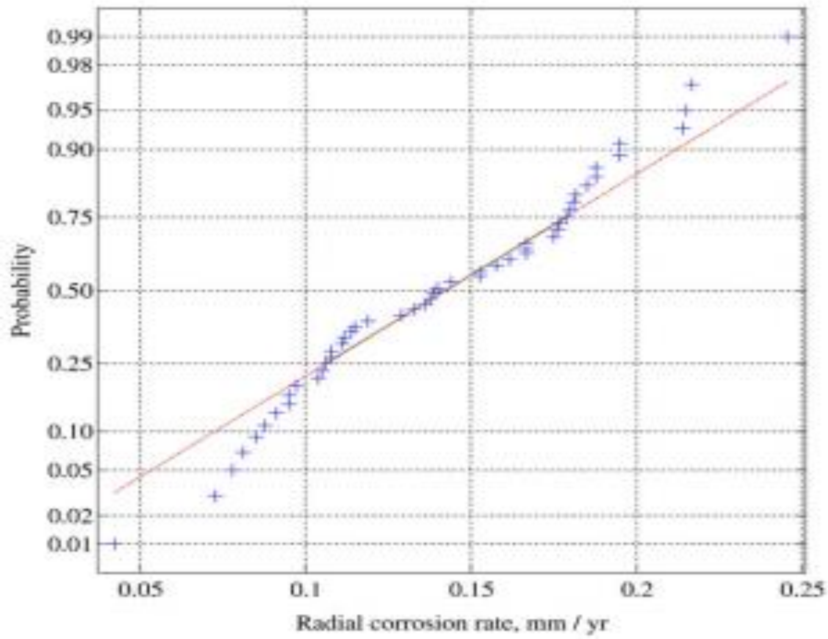

Figure 2.1: Radial corrosion on normal probability paper.

Source: Macdonald et.al.,2007

2.4.2 Gouges

A gouge result a metal loss defect which cause surface damage to pipeline due to contact with foreign object that scraped out the material out of the pipe (Macdonald and Cosham, 2005). It causes adverse effects on pipeline integrity, while it causes local stress and also strains concentration to the pipelines.

2.4.3 Dents

Dents in transmission pipelines are a permanent plastic deformation of circular cross section of the pipe. A dent is a gross distortion of the pipe cross section. Depth of dent is defined as a maximum reduction in the diameter of the pipe compared to the original diameter (Cosham and Hopkins, 2004).

According to statistical results the Office of Pipeline Safety of the U.S. Department of Transportation (DOT), from 1985 until 2003, there are about 28% incidents had been reported most of the cases related to the failures of pipeline caused by dents (Jacob *et.al*., 2010). There are several types of dents such as smooth dent, kinked dent, plain dent, unconstrained dent, and constrained dent. Smooth dent is caused by a smooth change in curvature of pipe wall. It contains a gouge is a very severe form of mechanical damage.

A smooth dent which containing gouge is lower than a burst strength of equivalent plain dent and lower than equivalent gouge in un-dented pipe (Cosham and Hopkins, 2004). The dent depths include both the local indentation and any divergence from the nominal circular cross section.

Kinked dent is a dent cause by abrupt change in curvature of pipe wall of the sharpest part of dents is less than five times the wall thickness (Cosham and Hopkins, 2004).

Plain dent is a smooth containing no wall thickness reductions such as gouge or crack or some other imperfections such as girth or seam weld (Cosham and Hopkins, 2004). It is not significantly reducing the burst strength of the pipe (Macdonald *et.al.*, 2007).

Unconstrained dent is a dent which elastically free rebound (spring back) when the indenter removed, and freely rebound as internal pressure changes (Cosham and Hopkins, 2004).

Constrained dent is a dent that not free to rebound or reround due to indenter is not removed. For example rock dent (Cosham and Hopkins, 2004). Constrained plain dents do not significantly reduce the burst strength of the pipe (Macdonald *et.al.*, 2007).

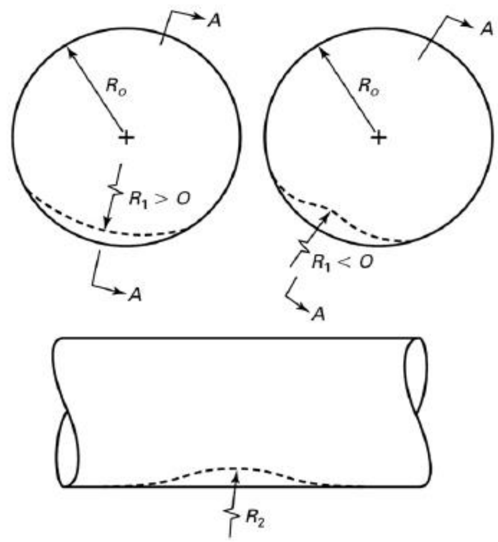

Figure 2.2: Dent geometry

Source: Jacob et.al., 2010

2.5 Codes and Standards

In pipeline industry, metal-loss corrosion is a common integrity threat. The prediction of burst pressure is most relevance to oil and gas industry (Zhou, 2012). The pressure of corroded pipes depending on the loading and scopes of the pipelines such as ASME B31G, DNV RP-F101, modified ASME B31G,PCORRC, RSTRENG, SHELL-92 and so on (Li *et al*., 2009). The semi-empirical methods based on measurement data which only consider the length and depth dimension of the simple, 2D geometrical shape are (ASME B31G), Modified ASME B31G, DNV and Advantica, which used to approximate the real corrosion failure (Fekete and Varga, 2012). Every codes are applied by considering various criteria of the test data for example ASME B31G, modified ASME B31G and RSTRENG are applicable for low, moderate, high tough steels. Meanwhile DNV-RP F101 and PCORRC are applicable for moderate to high toughness steels (Cosham et al., 2007).

	Pressure only		Combine loading	
	Length and depth	Area and depth	Pressure and bending	Area and depth
Coded method	ASME B31G			
	Modified ASME B31G			
	DNV F101	DNV F101	DNV F101	DNV F101
Other methods	RSTRENG	RSTRENG Effective	Bubenik FEM	
	Mok et. al	Leis.PCORRC	Safe-SwRi Stress model	
	Hopkins		Andrew correction factor	
	Rosenfeid		Wang-SwRi Strain model	
	Choi et al.		SINTAP	
	SINTAP			

Figure 2.3: Methods for corrosion assessment including codified and other methods

Source: Adib et.al., 2006

2.5.1 ASME B31G

American Society of Mechanical Engineers (ASME) B31G originally developed and published in 1984, it is being used widely in determine the remaining strength of corroded pipeline. For consideration of defect geometry, ASME B31G had proposes bulging factors. The flow stress based on researcher, X.Y.Xu et.al, it is not applicable for high strength steel such as x100.The researcher state that the application below is limited to evaluation of metal loss due to external or internal corrosion defect which have smooth contour with depth between 10% and 80%.

The calculation below involved the pressure failure and Folias factor of ASME B31G. Those parameters are included in List of Symbols.

From Eq.(2.1) until Eq.(2.5) are taken from researcher, Abid *et. al.*, 2006, while Eq. (2.6) until Eq.(2.9) taken from researcher L.Y.Xu.,2012. There are 2 different equations based on the type of defect which being concluded by researcher Abid *et. al.,* where Eq. (2.3) is significant only for a parabolic defect while Eq. (2.5) is applicable for rectangular defect.

$$P_f = \frac{2(1.1\sigma_y)t}{D}\left[\frac{1-\frac{2}{3}\left(\frac{d}{t}\right)}{1-\frac{2}{3}\left[\left(\frac{d}{t}\right)/M\right]}\right] \quad (2.1)$$

$$M = \sqrt{1+0.8\left(\frac{L}{D}\right)^2\left(\frac{D}{t}\right)} \quad (2.2)$$

For $\sqrt{0.8\left(\frac{L}{D}\right)^2\left(\frac{D}{t}\right)} \le 4$ Parabolic defect (2.3)

$$P_f = \frac{2\left(1.1\sigma_y\right)t}{D}\left[1-d/t\right] \text{ where } M = \infty \quad (2.4)$$

For $\sqrt{0.8\left(\frac{L}{D}\right)^2\left(\frac{D}{t}\right)} > 4$ Rectangular defect (2.5)

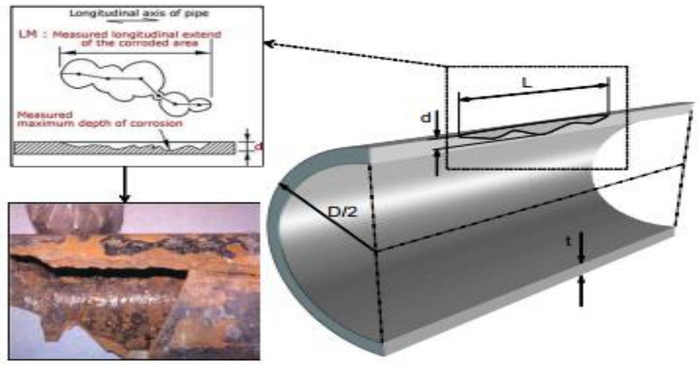

(a)

(b)

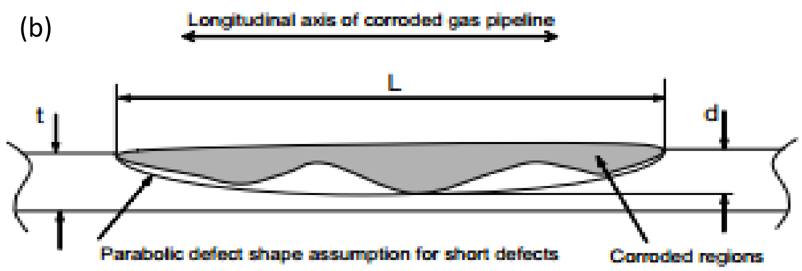

(c)

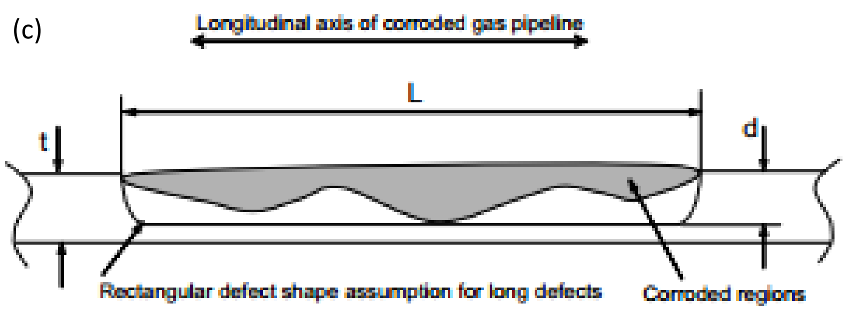

Figure 2.4: (a) Typical illustration of corrosion defects in longitudinal axis of pipe, **(b)** short corrosion defect simplified as a parabolic curve, **(c)** long corrosion defects simplified as a rectangular defect based on ASME B31G code

Source : Abid *et. al*., 2006

$$S_{flow} = 1.1 \times SMYS \tag{2.6}$$

$$M = \sqrt{1+0.8z} \ , \ z = \frac{L^2}{Dt} \tag{2.7}$$

For z ≤ 20

$$P_f = S_{flow} \frac{2t}{D} \left[\frac{1 - \frac{2}{3}\left(\frac{d}{t}\right)}{1 - \frac{2}{3}\left(\frac{d}{t}\right)\frac{1}{M}} \right] \tag{2.8}$$

For z > 20

$$P_f = S_F \frac{2t}{D}\left(1 - \frac{d}{t}\right) \tag{2.9}$$

2.5.2 Modified ASME B31G

Pressure failure and Folias factor for modified ASME B31G. Those parameters are shown in List of Symbols.

From Eq.(2.10) until Eq.(2.12) are taken from researcher, Abid *et. al*.,2006 while Eq.(2.13) until Eq.(2.16) taken from researcher L.Y.Xu.,2012.

$$\sigma_f = 1.1\sigma_y + 69MPa \tag{2.10}$$

$$P_f = \frac{2(1.1\sigma_y + 69)t}{D} \left[\frac{1 - 0.85\left(\frac{d}{t}\right)}{1 - 0.85\left[\left(\frac{d}{t}\right)/M\right]} \right] \tag{2.11}$$

For $\left(\frac{L}{D}\right)^2 \left(\frac{D}{t}\right) \le 50$

where

$$M=\sqrt{1+0.6275\left(\frac{L}{D}\right)^{2}\left(\frac{D}{t}\right)-0.003375\left(\frac{L}{D}\right)^{4}\left(\frac{D}{t}\right)^{2}}\leq 4 \qquad (2.12)$$

$$S_{flow}=SMYS+69MPa \qquad (2.13)$$

$$P_{f}=S_{flow}\frac{2t}{D}\left[\frac{1-0.85\left(\frac{d}{t}\right)}{1-0.85\left[\left(\frac{d}{t}\right)/M\right]}\right] \qquad (2.14)$$

$$z=\frac{L^{2}}{Dt} \qquad (2.15)$$

$$M=\sqrt{1+0.6275z-0.003375z^{2}}$$

For z > 50

$$M=0.032z+3.3 \qquad (2.16)$$

2.5.3 DNV-RP-F101

Det Norske Veritas (DNV) also known as DNV-RP-F101 is the first comprehensive and extensive code, recommended practice for assessing corroded pipelines under combined internal pressure and longitudinal compressive stress (Netto *et al.*, 2005). Besides, DNV-RP-F101 is a method to evaluate corroded pipelines under complex condition such corrosion induce defect and longitudinal compressive and bending loads due to soil movement (Xu and Cheng, 2012). DNV capable to assess pipelines which containing a single defect, multiple interacting defects and complex shapes defects. Based on model in source (Xu and Cheng, 2012), isolated corrosion defect under pipeline internal pressure has been considered, with defect depth not exceeding 85% of wall thickness.

Pressure failure and Folias factor of DNV-RP-F101.

Those parameters are shown in List of Symbols.

From Eq.(2.17) until Eq. (2.18) are taken from researcher, Abid *et. al.*,2006, while Eq. (2.19) until Eq. (2.10) taken from researcher L.Y.Xu.,2012 .

$$P_f = \frac{2(\sigma_U)t}{D-t}\left[\frac{1-\left(\frac{d}{t}\right)}{1-\left[\left(\frac{d}{t}\right)/Q\right]}\right] \tag{2.17}$$

$$Q = \sqrt{1+0.31\left(\frac{1}{\sqrt{Dt}}\right)^2} \tag{2.18}$$

$$P_f = \frac{2t}{D-t}SMTS\left[\frac{1-\left(\frac{d}{t}\right)}{1-\left(\frac{d_1}{tQ}\right)}\right] \tag{2.19}$$

$$Q = \left(1+0.31\frac{L^2}{Dt}\right)^{1/2} \tag{2.20}$$

2.5.4 RSTRENG

Remaining Strength of the Corroded Pipe is one of the coded methods for assessing detrimental effect of surface corrosion defects on the burst pressure of pipeline (Tanguay *et.al*., 2008)

.

2.5.5 Shell-92

Shell-92 model is suitable to predict failure of pipeline when service time exceeds 10 years. Prediction of Shell-92 is safer compared to B31G model (Li *et. al.,* 2009).

2.5.6 Choi et.al method

Choi *et.al.*, has been proposed a limit loads a function of R/t, d/t, $L/\sqrt{Rt}$ and based no limit load analysis assumptions and finite analysis of corroded pipelines.

Those parameters being shown in List of Symbols.

From Eq.(2.21) until Eq.(2.22) are taken from researcher, Abid *et. al*., 2006.

$$P_f = \begin{cases} 0.9\dfrac{2(\sigma_U)t}{D_i}\left[C_O + C_1\left(\dfrac{L}{\sqrt{Rt}}\right) + C_2\left(\dfrac{L}{\sqrt{Rt}}\right)^2\right], \dfrac{L}{\sqrt{Rt}} < 6 & (2.21) \\ 1\dfrac{2(\sigma_U)t}{D_i}\left[C_3 + C_4\left(\dfrac{L}{\sqrt{Rt}}\right)\right], \dfrac{L}{\sqrt{Rt}} \geq 6 & (2.22) \end{cases}$$

where

$$\left\{C_0 = 0.06\left(\frac{d}{t}\right)^2 - 0.1035\left(\frac{d}{t}\right) + 1, C_1 = -0.6913\left(\frac{d}{t}\right)^2 + 0.4548\left(\frac{d}{t}\right) - 0.1447,\right.$$

$$\left.C_2 = 0.1163\left(\frac{d}{t}\right)^2 - 0.1053\left(\frac{d}{t}\right) + 0.0292, C_3 = -0.9847\left(\frac{d}{t}\right) + 1.1101, C_4 = 0.0071\left[\frac{d}{t}\right] - 0.00126\right\}$$

2.5.7 SINTAP

SINTAP is known as Structural Integrity Assessment Procedure for European Industry. This procedure is used to investigate for the structural integrity assessment of corroded pipelines (Abid *et.al*., 2006). Besides, SINTAP offered a failure assessment diagram (FAD). FAD method, 'interpolating curve' or failure curve is used to assess failure zone, safe zone and safety zone. A typical failure assessment diagram is shown in Figure 2.5 below. This failure assessment diagram accounts for plastic collapse and also brittle failure which includes of safety factor considerations.

The failure assessment diagram take accounts on the normalized stress intensity factor versus normalized stress or loading parameter (Abid *et. al*.,2006). SINTAP procedure is divided into several distinct levels. It can be prove through some mathematical expression of the SINTAP default level with a aforementioned assumption as written below (Abid *et. al*.,2007):

$$f(L_T) = \left[1 + \frac{L_T{}^2}{2}\right]^{-\frac{1}{2}} \left[0.3 + 0.7 \times e^{\left(-0.6 \times L_T{}^6\right)}\right] \quad (2.23)$$

For $0 \leq LT \leq 1$,

Where f (L_T) is a plasticity correction, L_T as non-dimensional loading or stress -based parameter and σ_y yield stress.

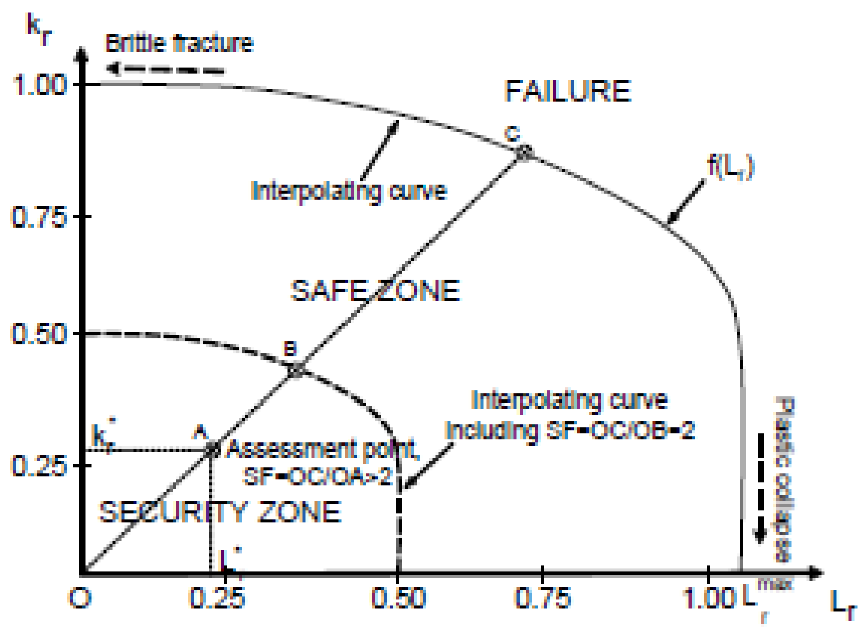

Figure 2.5: Typical presentation of failure assessment diagram (FAD) for a crack

Source : Abid *et. al*., 2007

2.6 FAILURE IN PIPELINE

2.6.1 Hydrogen Induce Cracking (HIC)

Damage of hydrogen can be called as hydrogen induced cracking (HIC), hydrogen induced blistering cracking or stepwise cracking. About 25% of equipment failures caused by hydrogen damage had been indicated in the inspection program (Xu and Cheng, 2012). Expositions of steel to the aqueous H2S environment absorb atomic hydrogen produced on a surface by the H_2S corrosion reaction. During penetration of hydrogen atoms into steel and precipitate in the matrix-inclusions interfaces, significant cracking may occur in low medium strength, low alloy steels commonly used for pressure vessels and piping in the oil and chemical industries (Domizzi *et.al.,* 2001). HIC usually occurs in low strength, low carbon steels used in pipelines and pressure vessels carrying wet sour hydrocarbons (Venegas *et.al.*, 2011). The crack associated with elongated sulphide is illustrated in Figure 2.6.

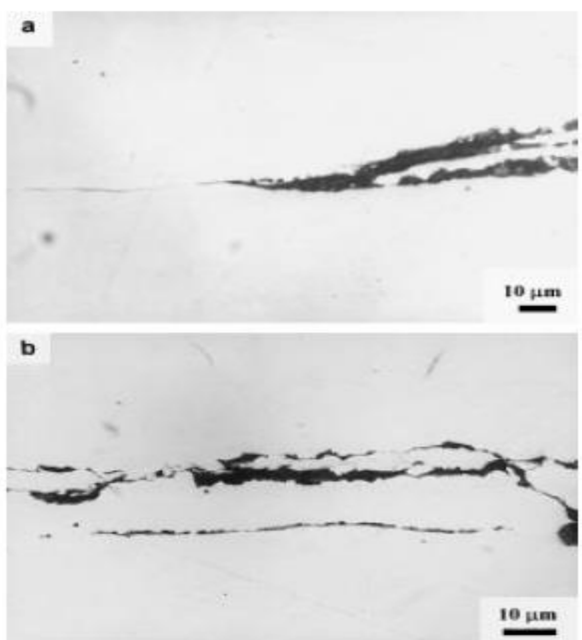

Figure 2.6: Crack associated with elongated sulphide

Source: Domizzi *et.al.*, 2001

2.6.2 Stress Corrosion Cracking (SCC)

Stress corrosion cracking (SCC) is cracking due to a process involving conjoint corrosion and straining of metal due to applied stresses. Significant failures have caused due to SCC in natural gas pipelines in Canada, which seriously affected consequences for the environment and the economy. Major causes of failure pipeline are due to involved high pH (~9.0) SCC (Cheng, 2007). SCC failure happened when mechanical stress and involving of interaction of corrosion produced a failure by cracking. Nowadays, stress corrosion cracking is highly important issues in oil and gas transmission pipelines used in oil and gas industries because of leakage or rupture and failure of the pipeline have a huge potential threat to environments and humans (Meresht *et.al.*, 2011).

Oxidation is a general term in representing the process of losing electron from metal, which can activate dissolution of bare metal or surface film forming/covering, or film thickening. Based on the concept proposed by Shoji et al., the combination of certain circumstance such as combination of material, environment, loading conditions for SCC systems, the enhancement of crack tip oxidation can realized through either physical degradation mode, physical chemical degradation mode or both as illustrated in Figure 2.7 (Shoji *et.al.*, 2010). If the oxide film degradation frequency is high, the physical degradation effect would be more significant, as the result of high crack tip strain rate and low oxide film toughness. Based on Figure 2.7 illustrated below, the stage I, enhanced oxidation reaction of the crack tip material, stage II is about the formation or growth (recovery) of the protective film, stage III is a steady oxidation state (Shoji *et.al.*, 2010).

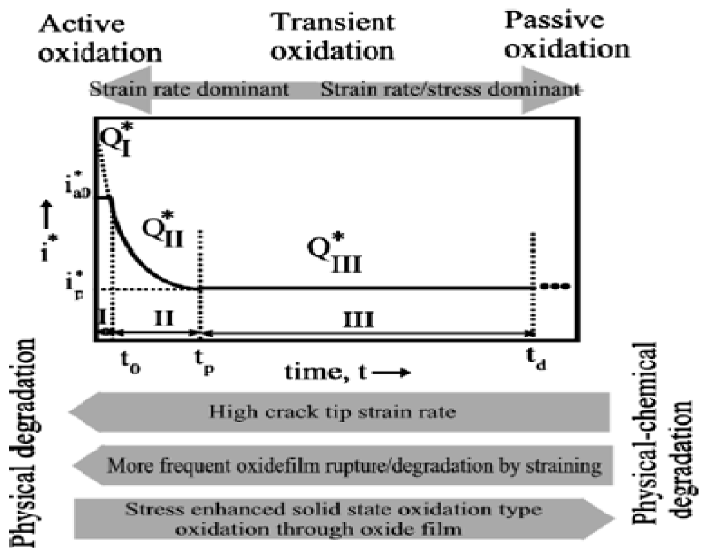

Figure 2.7: Schematic of stress corrosion cracking sub-processes

Source: Meresht *et al.*, 2011

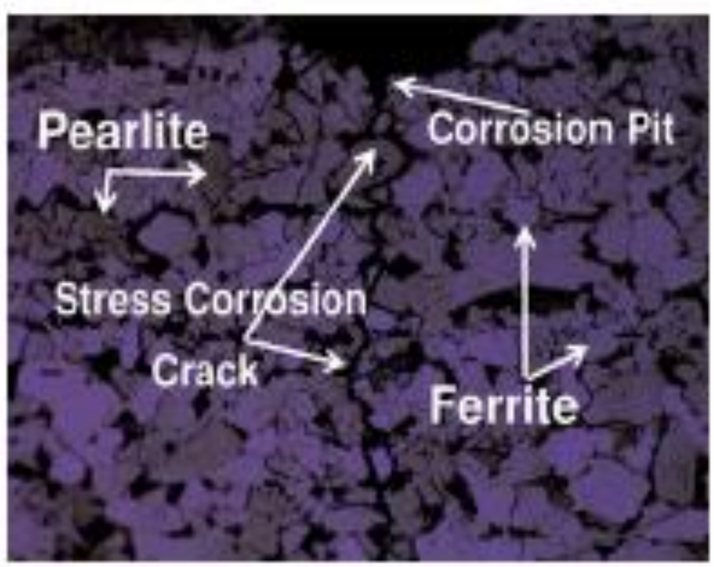

Figure 2.8: The optical microscopic image of the stress corrosion cracking (x200).

Source : Meresht *et al.*, 2011.

2.7 METHODS TO PREVENT CORROSION IN PIPELINES

Pipeline made up from good material with good safety record due to the combination of good design and operating practice. However, aging occasionally fail the structure of the pipeline. National Association of Corrosion Engineers (NACE) recommended some method in controlling the corrosion in order to protect the corrosion in oil and gas pipelines.

2.7.1 Cathodic Protection (CP)

Cathodic protection (CP) is a method to control corrosion by using a direct electrical current which neutralizes external corrosion typically associated with metal pipe. It is commonly used during pipeline is buried in water or underground. The cathodic may prevent pipeline from corrode when executed on a new pipe. Cathodic protection can impede existing corrosion of the line on an older pipeline.

2.7.2 Coating and Linings

Coatings and linings are applied to pipelines whether above or below ground and often are used in combination with cathodic protection.

2.7.3 Corrosion Inhibitors

Corrosion inhibitors are compounds which when added to the upstream pipeline can inhibit the corrosion of carbon and low-alloy steels which are commonly used because of their cost effectiveness.

2.7.4 Pipeline material

Pipeline material used will also significantly influence corrosion. Using materials like plastic, stainless steel or special alloys can enhance the lifetime of the pipeline, while steel or steel reinforced concrete is subject to corrosion.

CHAPTER 3

METHODOLOGY

3.1 INTRODUCTION

This chapter will describe about the procedures analysis on the assessment on effect of geometry defect for steel pipe. The research methodology is a set of procedures or methods used to conduct research. Methodology is needed for a guideline in order to ensure the results are accurate based on the objective. Type research that will be used in determining the effect crack on pipeline is quantitative methodologies. There are several steps need to be followed to ensure the objective of the research can be achieved starting from finding literatures until submitting the final report.

3.2 FLOW CHART OF METHODOLOGY

Flowchart represents a process by showing the steps as box of various kinds, and their order by connecting with arrows. Flowchart is important in doing research by helping the viewer to understand a process flow and help to visualize what is going on. Flow chart methodologies were constructed related to the scope of product as a guided principal to formulate this research successfully, in order to achieve the objectives of the project research. This is important to ensure the research experiment is on the right track. The terminology of work and planning for this research was shown in the flow chart Figure 3.1.

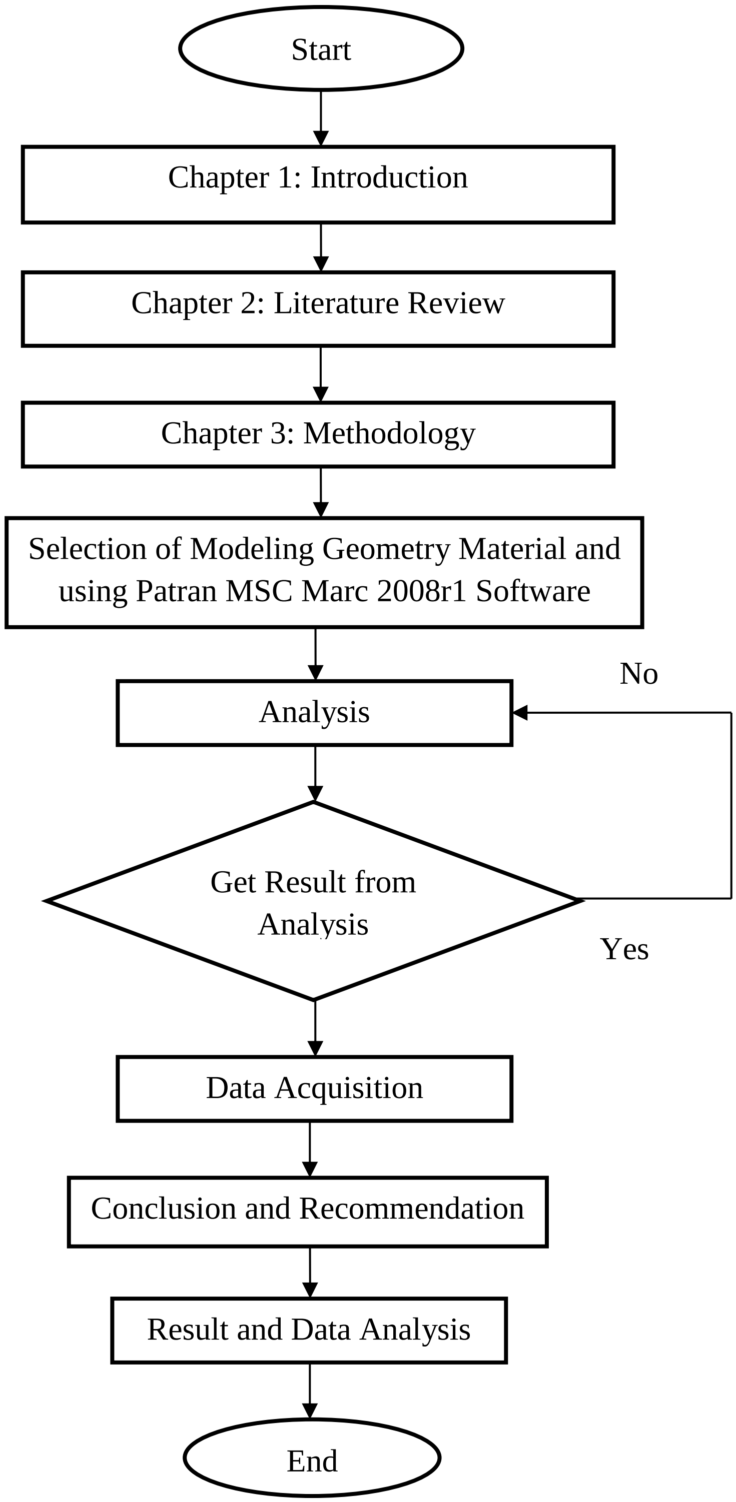

Figure 3.1: Overall Flowchart Research

3.3 PROCEDURE

The complete procedure to analyze effect of geometry defect for steel pipe is shown as in Figure 3.2. It consists of overall modeling design until analysis of the result.

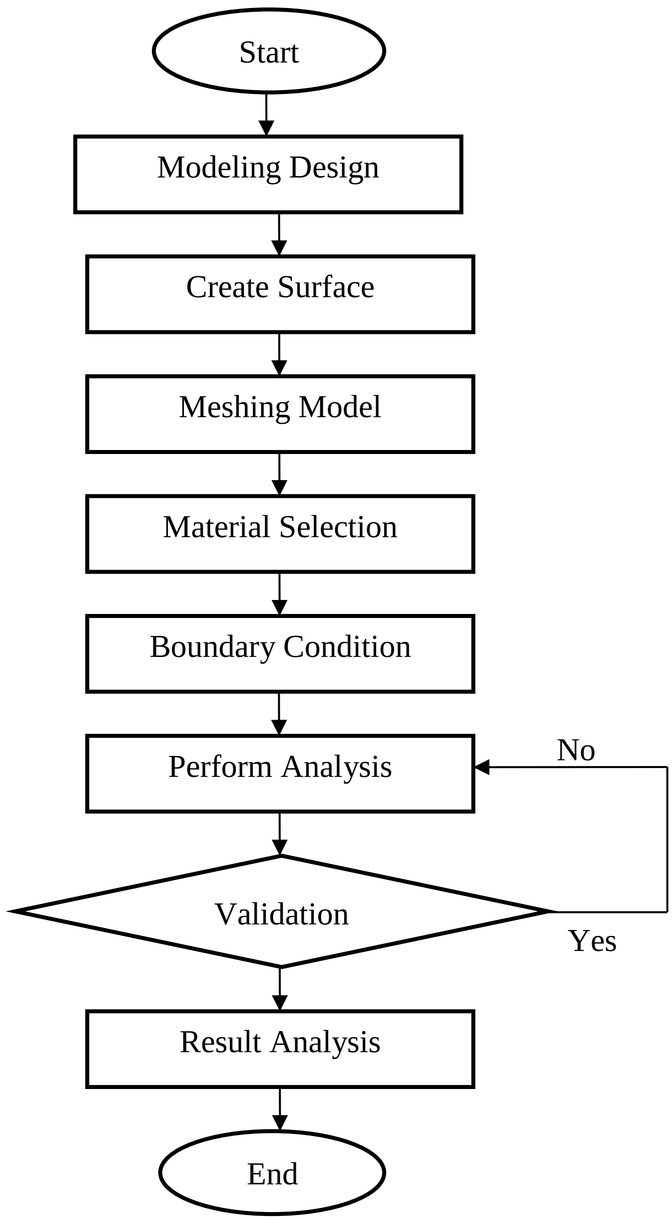

Figure 3.2: Methodology Flowchart

3.3 FINITE ELEMENT ANALYSIS (FEA)

MSC Marc PATRAN 2008r1 provides an easy way for user to simulate the complex shape for analysis process. There are some material behavior being include in this software, where there mixture model allow the users to define a composite material consists for membrane, shell and continuum element type. Besides, MSC Marc PATRAN 2008r1 also has capability to automatically split up the mesh during the analysis. The mesh can be done at nodes and along element edges (2-D and shells) or element faces (3-D). The meshing size can be control using mesh seed before mesh is applied towards the model.

Furthermore, using FEA will reduce the time and cost for prediction. The MSC Marc PATRAN 2008r1 can applied boundary condition of the material which need to be analyse, it is easy to conduct. The data result provided various option such as displacement, stress, strain, and many more. The MSC Marc PATRAN 2008r1, help researchers and design engineering field in predict the behavior of the model without taking any neither expensive budget nor time.

3.4.1 Modelling Design

The defect of rectangular shape and groove shape were designed using MSC Marc PATRAN 2008r1 software. About 18 designs with various shapes and defect were simulated. Firstly, as displayed in Figure 3.3, turn on Patran software, choose New Database and rename the ‘file name’ before click on ‘Apply’. Select MSC.Marc for analysis code as to simulate the defect. Click on Preference and choose ‘Geometry’ while select the geometry scale factor as a millimeter. The selection of geometry displayed in Figure 3.4.Then the analysis begin to started.

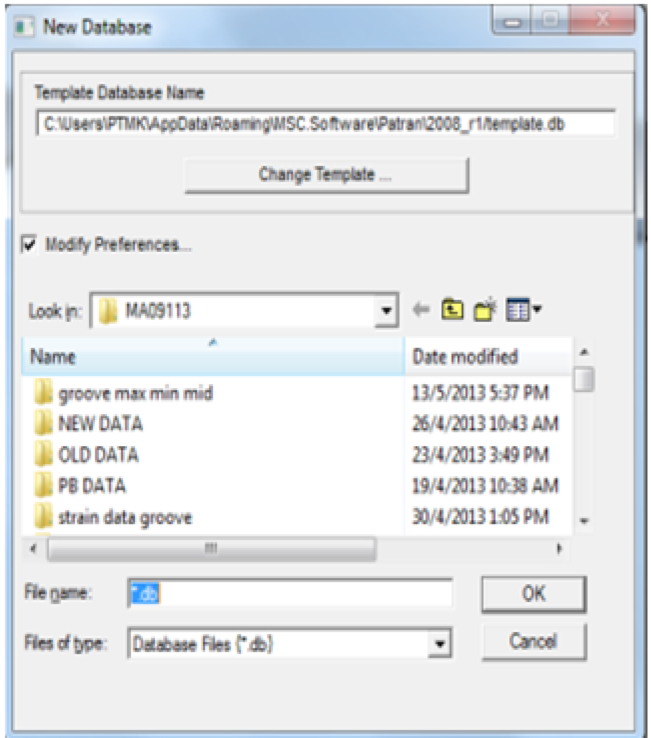

Figure 3.3: Select New Database

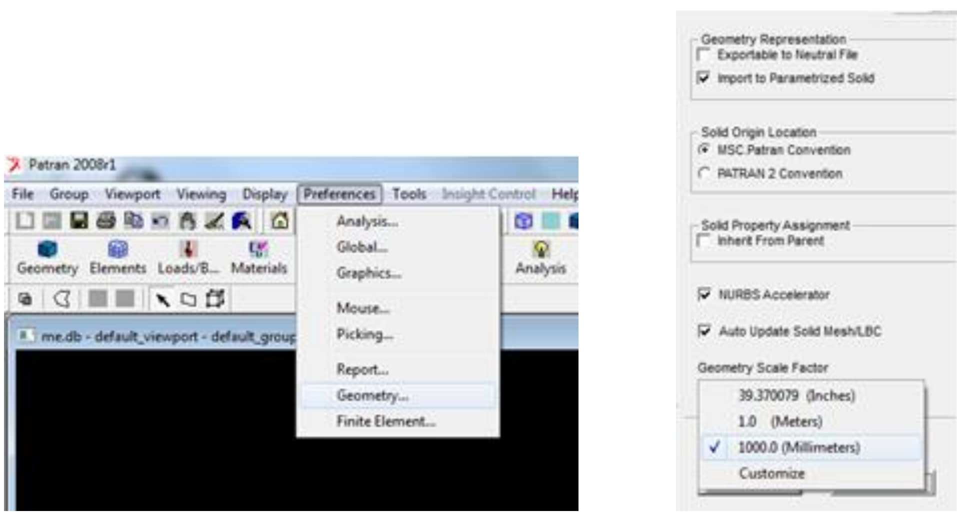

(a) (b)

Figure 3.4: Geometry selection. (a) Select Preference tab (b) Geometry Scale factor

3.4.2 Geometry

Half of pipe size model used to be analyzed using MSC Marc 2008r1 software. The parameter for outer diameter, D of pipe is 60.5mm and the thickness, t of the pipe about 4 mm. This research more focus on the effect of geometry defect upon the pipe, where two type of defect such as rectangular-shaped defect and groove-defect are used. This research is to verify the effect defect over shape and width on corrosion defect incorporating stress-based criteria. The analysis considered width groove-shaped defect, d_g = 0.2, 0.5 and 1mm, and the width rectangular-shaped defect, w_c = 0.2, 0.5 and1 mm. The finite element models constructed into three different depths for pipe configurations a/t = 0.2, 0.5and 0.75.

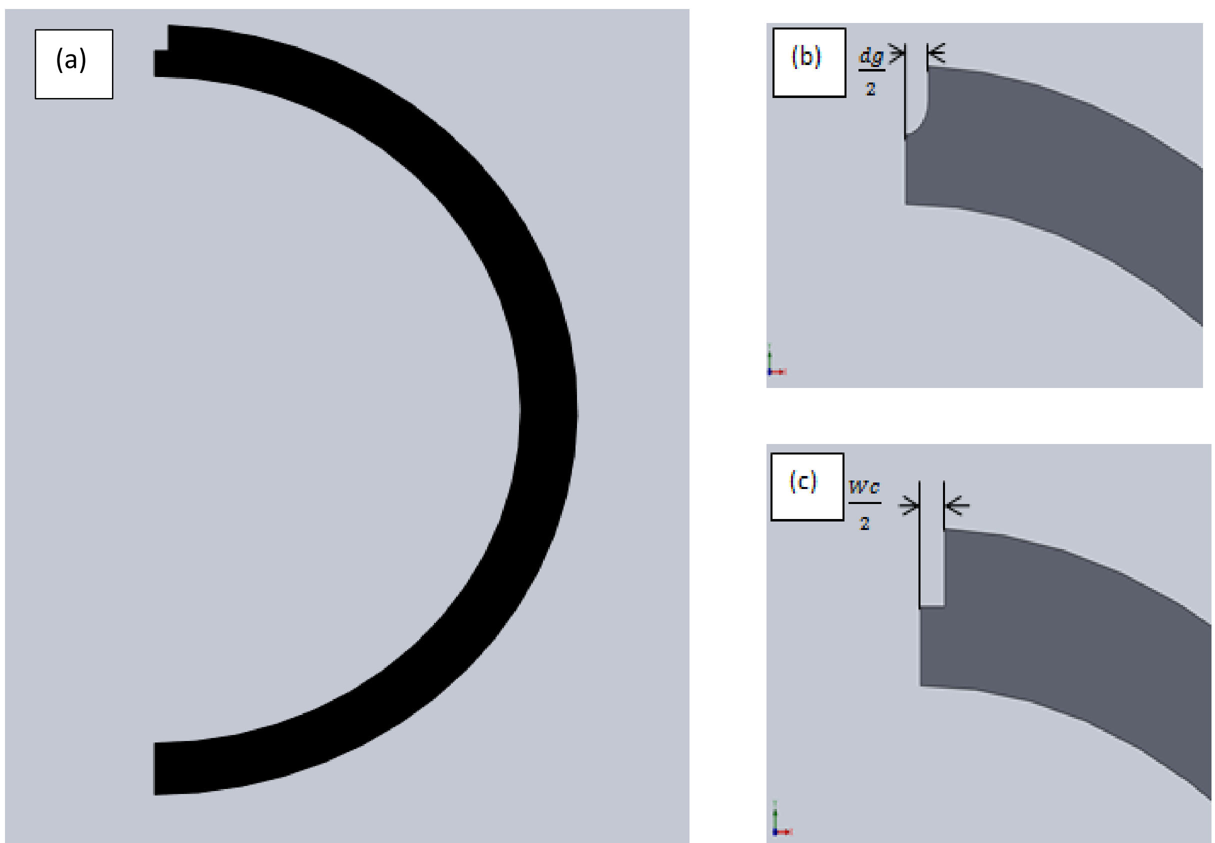

Figure 3.5 (a) Half pipe model for analyzed with a/t = 0.5; (b) Groove shaped-defect; (c) rectangular-shaped defect

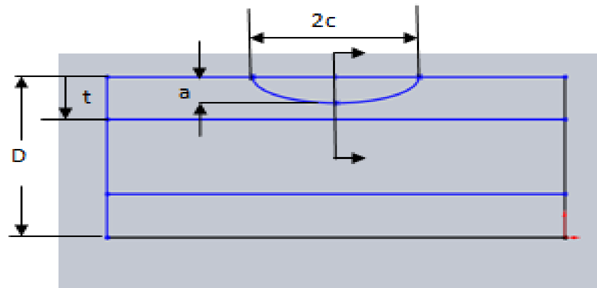

(a)

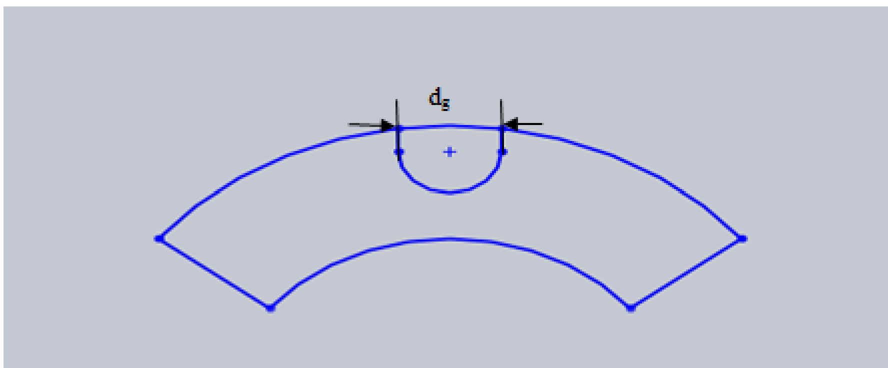

(b)

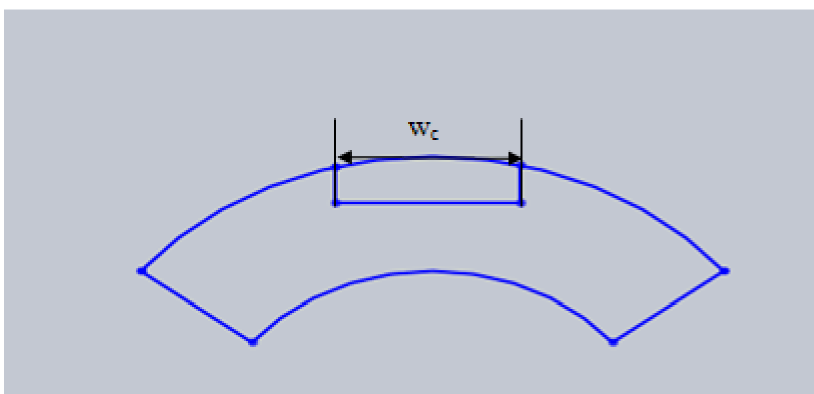

(c)

Figure 3.6: Pipe configuration and defect geometry employed in the analyses

Type of defect and cracks will be summarized in Table 3.1. The parameter varied in the model shown in Figure 3.3 (b), (c) and Figure 3.4 is described as below:

- Outside diameter, *D*
- Pipe wall thickness, *t*
- Angular shape defect with defect width, w_c
- Groove shape defect with groove width, d_g
- Corrosion defects with fixed depth, *a*
- Varying corrosion length, *2c*

Table 3.1: Geometry parameters of groove defect and rectangular defect

Diameter of pipe, *D* = 60.5mm, wall thickness, *t* = 4mm			
Case	Thickness defect (%)	Groove width, d_g (mm)	Rectangular defect, w_c (mm)
1	20	0.2	0.2
2		0.5	0.5
3		1	1
4	50	0.2	0.2
5		0.5	0.5
6		1	1
7	75	0.2	0.2
8		0.5	0.5
9		1	1

- 20% depth defect (shallow defect)
- 50% depth defect (moderately defect)
- 75% depth defect (deep defect)

Finite element method is widely used to study crack defects and to predict the stress intensity, especially for elastic-plastic analysis. In this study, the finite element program MSC Marc 2008r1 was to model defects and prediction of failure pressure. The factor geometry selected was millimeter. Half size of the pipe is created by chosen origin coordinate [0, 0, 0]. The other coordinate been created such as [0, 26.25, 0], [0, 30.25, 0] and so on. Curve is created to connect each node by select Action: Curve, Object: Point. Point used to created straight line while for 2D Arc2Point used for curve shape. The break interaction was used to break the line between two curves. Angle of 10^{o} created away from defect shape due to focus area of the defect. After the defect created and the nodes being attached together as needed shape, next procedure is to create smooth shaded upon the half pipe The geometry tab need to be chosen and select Action: Create, Object: Surface, Method: Curve. Then select two curve and 'APPLY'. The detail explanations above are shown in Figure 3.5 and Figure 3.6. Furthermore, setup vector direction of the surface to the positive z-axis as shown in Figure 3.7.

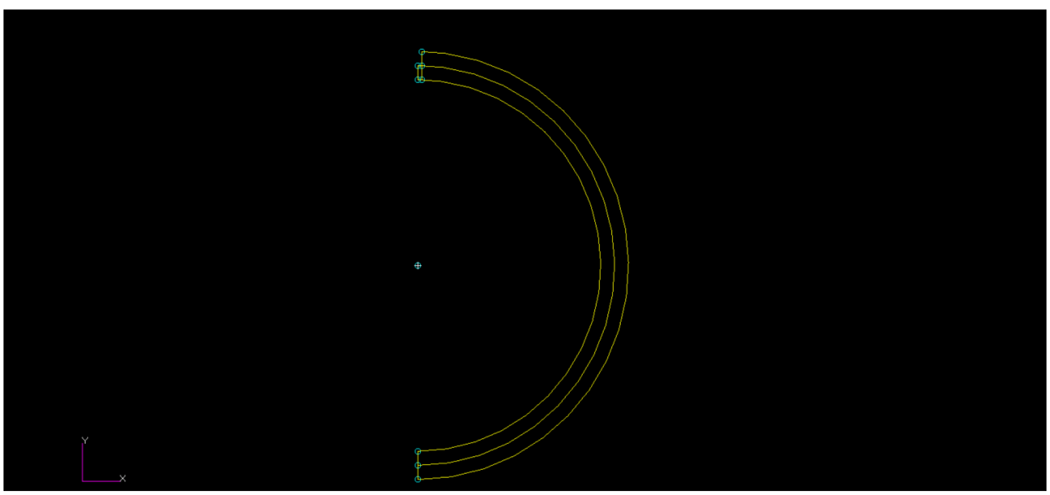

Figure 3.7: Creating nodes and curve line

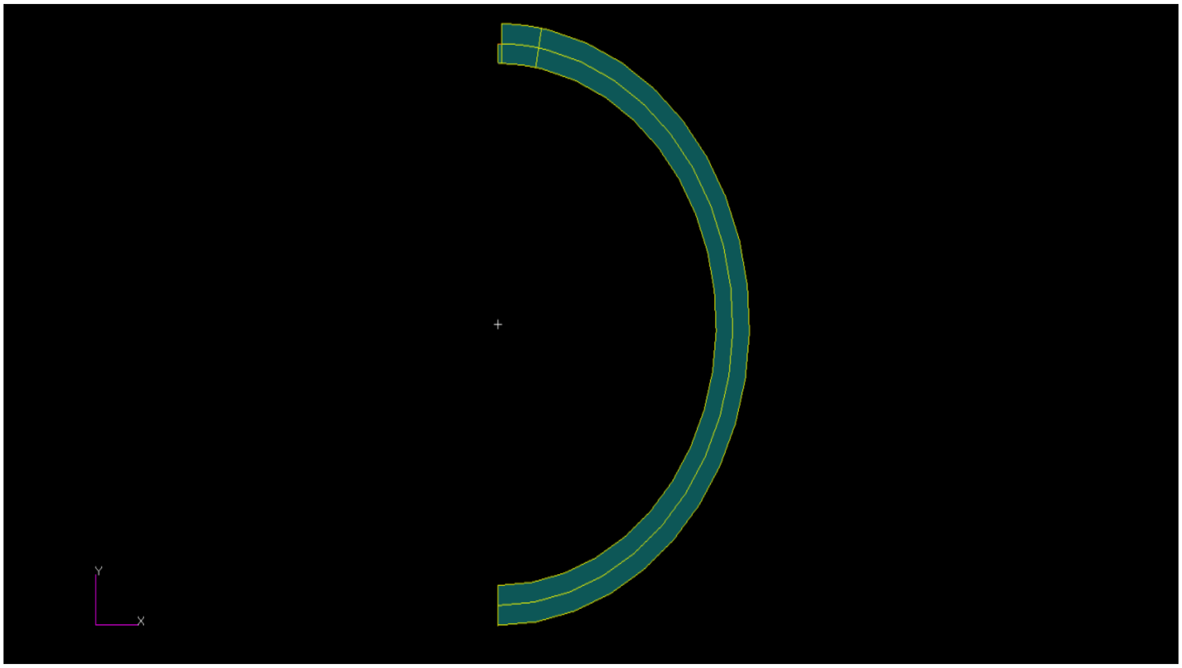

Figure 3.8: Creating defect and smooth shaded

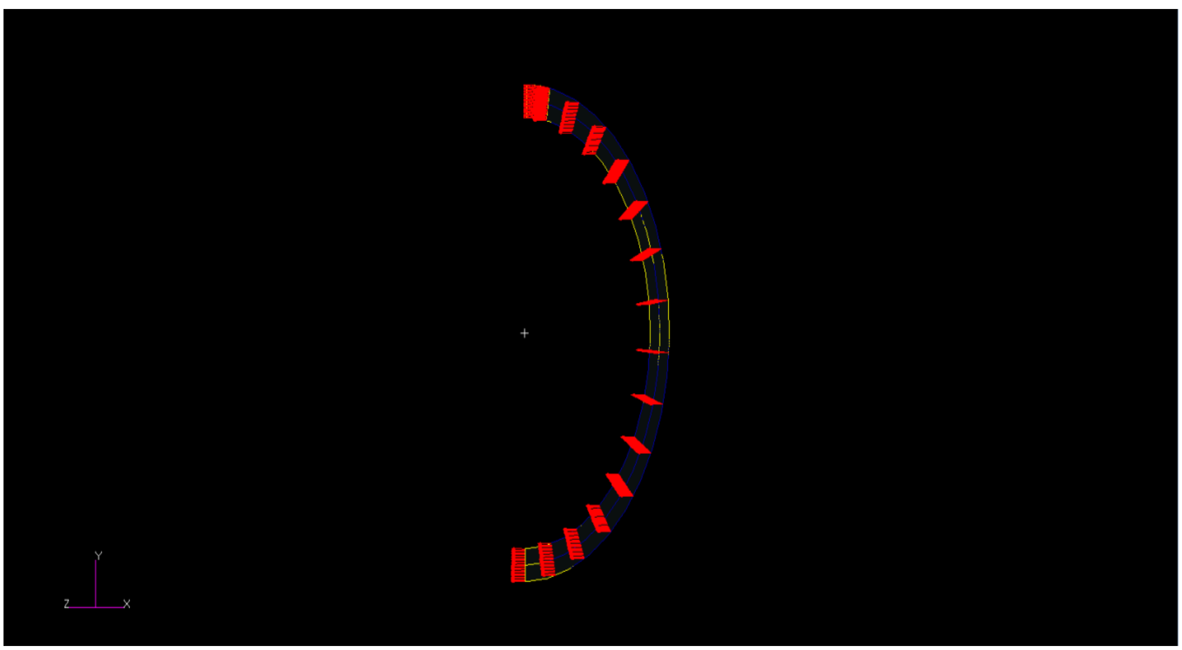

Figure 3.9: Direction of vector

3.4.3 Elements

In meshing, firstly, pick some surface or curves which need to be applied for the mesh seed. Create mesh seed definition for a given curve, or an edge of a surface or solid, with a uniform element edge length specified either by a total number of elements or by a general element edge length. The mesh seed will be represented by small yellow circles and displayed only when the Finite Element form is set to creating a Mesh, or creating or deleting a Mesh Seed.

There are a few types of mesh seed provided such as uniform, one-way bias and two-way bias. One way bias is to neither concentrate at the end of crack whether left nor right. Meanwhile, two way-bias is used to concentrated on both of the end of crack. The uniform mesh seed is used in this simulation. The mesh seed need to be very fine in defect area as to get accurate result for the focus area. Selection of mesh seed and mesh are clearly shown in Figure 3.7 and Figure3.8. Uniform type is choosing to FEA model.

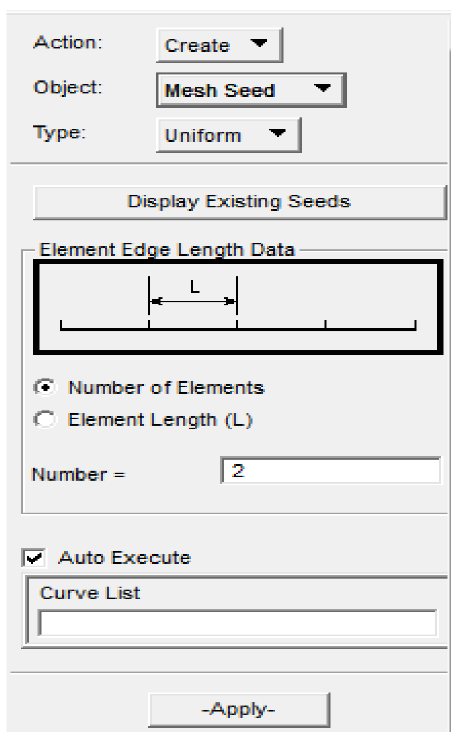

Figure 3.10: Creating mesh seed

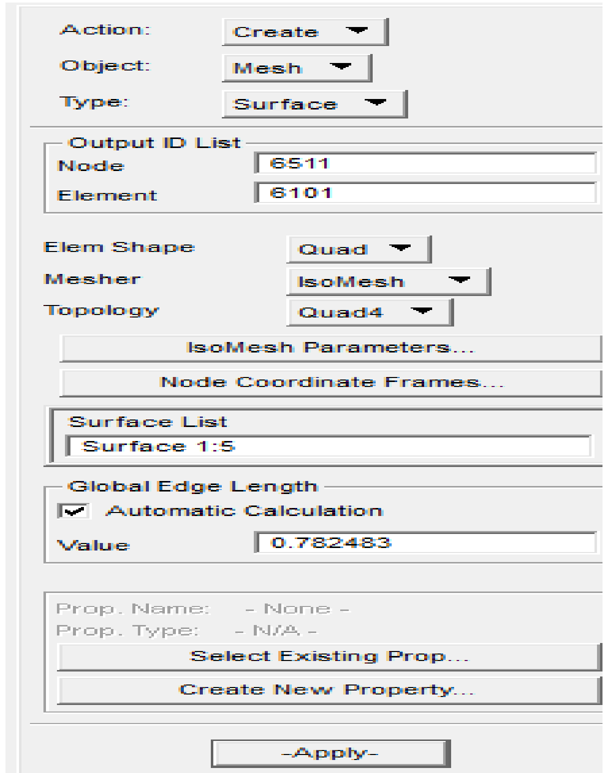

Figure3.11: Creating mesh

After meshing process, the most important thing is to equivalence the geometry. Equivalence used to reduce all nodes which coexist at a point to a single new node point. Equivalence will removed duplicate nodes which match from both sides of surface. To setup the equivalence is shown in Figure 3.9 below.

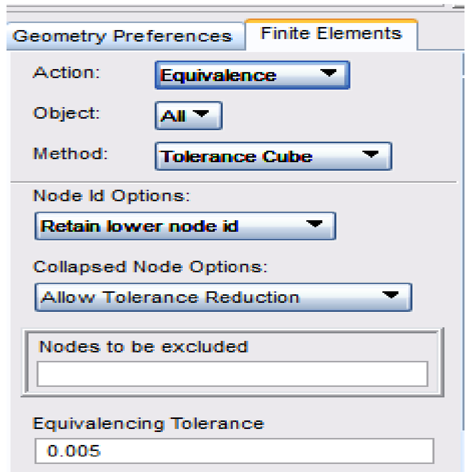

Figure 3.12: Select equivalence

3.4.4 Load/Boundary Conditions

The displacement and pressure were applied on the geometry in order to get the pressure effect on the surface of the quarter pipe. The new set name was renamed as 'symmetry' in setup the displacement. The translation data inserted as <0, , > because the x-axis is fixed. The curve of the pipe is selected as to apply the symmetry boundary. The needed curve was selected. Symmetry condition used to reduce the computational time, hence only half of the pipe containing defect was modeled. Meanwhile, 'pressure' was renamed to setup pressure on the simulation design. The pressure was applied at inner diameter of the pipe until it tends to reached burst pressure, the entire inner curves are selected as to apply pressure. Figure 3.10 shows the displacement and pressure which been applied to the pipe surface.

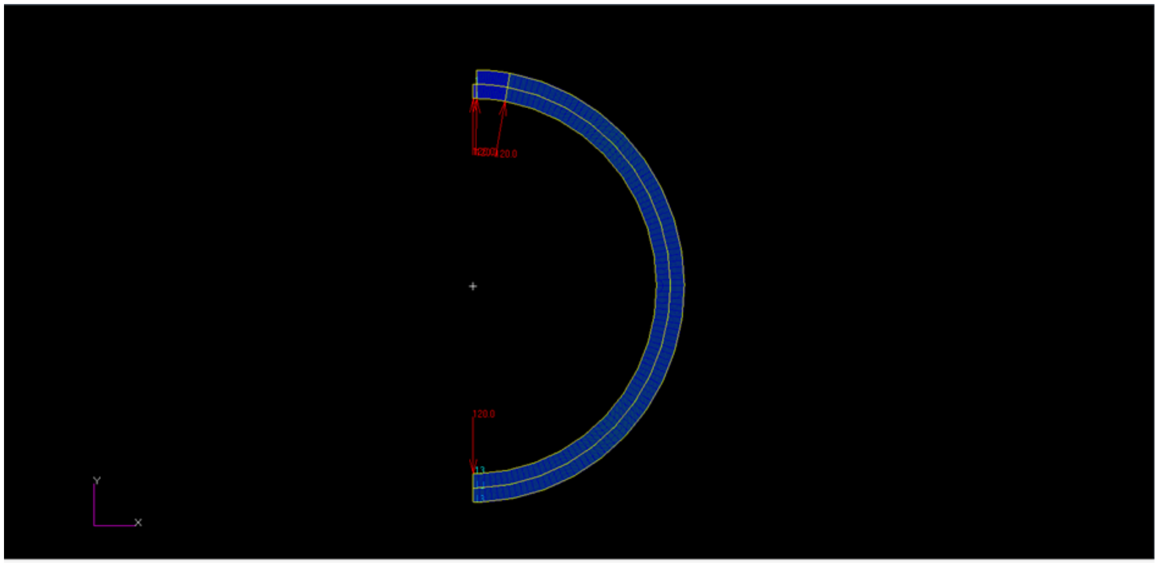

Figure3.13: Applied Displacement and Pressure

3.4.5 Define Material

The finite element analyses consider the type of material properties of the steels. The material properties of steel are inserted into the FEA analysis. The details of the mechanical properties of the steels are expressed in Table 3.3. After inserted the steel properties, click button apply. Imported the material grade B data through Field tab, tick the strain box and material grade B is imported from the file needed. The strain result taken from the experimental data of material grade B. For the constitutive model, plastic is chosen and it is being applied.

Table 3.2: Mechanical properties of pipeline steel

Mechanics Properties	**Steel (API 5L L245)**
Young's modulus (MPa)	207000
Poisson's ratio	0.3
SMYS (MPa)	326
SMTS (MPa)	465

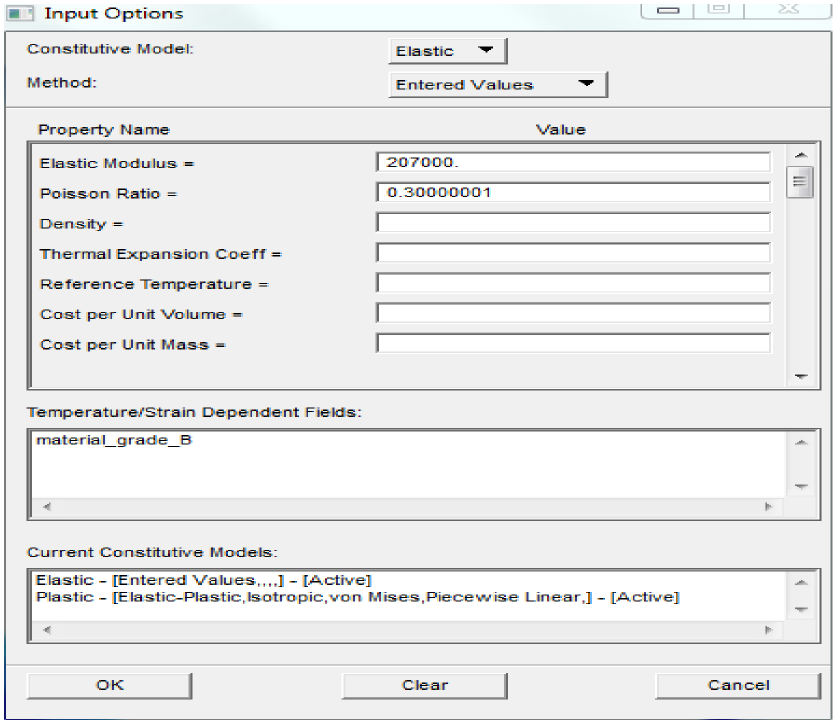

Figure 3.14: Elastic and Plastic Properties

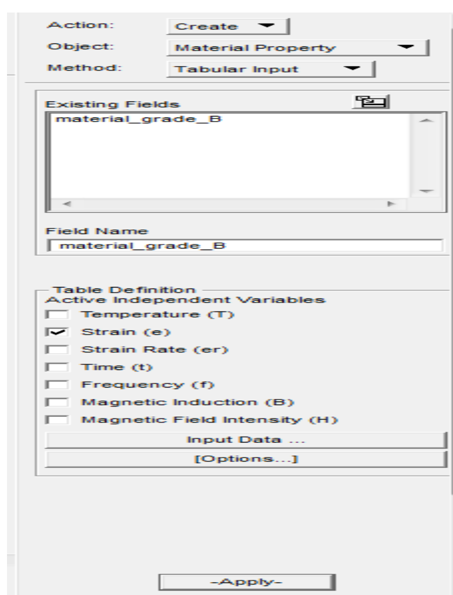

Figure 3.15: Creating Fields

3.4.6 Element 3D Properties

In element properties, select material and choose application region. Entire surfaces of the pipe need to choose to synchronize the material selected. In object, choose 2D and for the type as 2D Solid. Rename the Property Set Name as ‘steel’ and click button ‘apply’.

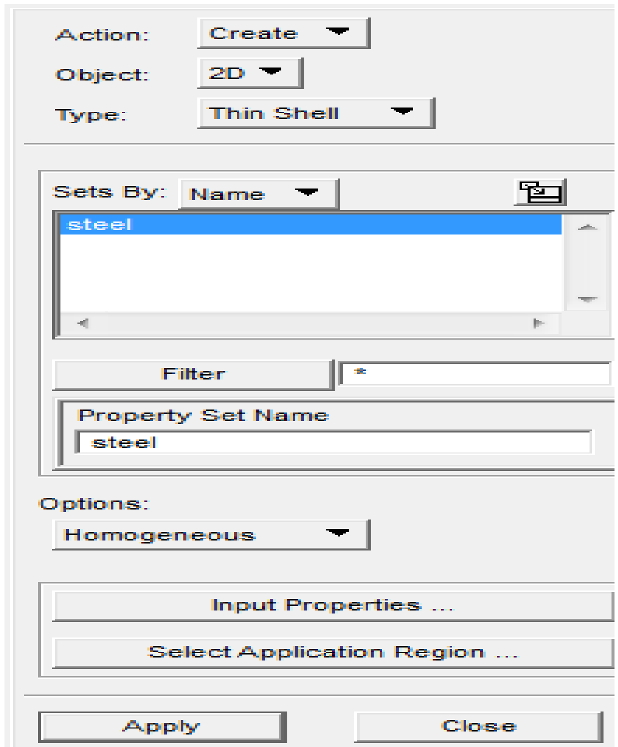

Figure 3.16: Setup Material properties

3.4.7 Analysis

As to analyze, the object and method need to setup as Object: Entire Model, Method: Analysis Deck. The code need to ensure to be MSC. Marc. Meanwhile, click on job parameters, click on Solver/Option and tick on Non-Positive Definite. Select Load Step Creation, tick on Follower Forces. Procceed with the Iteration Parameters. Change the value on the relative residual force: 0.001 and click 'OK'. The residual force is change to be 0.001 in order to get more accurancy and exact result.

After all analysis setup properly, run command prompt to ensure the result of the geometry model using MSC. Marc can run successfully. The command for MSC Marc PATRAN 2008 r1 is *"run_marc -j filename.dat -b n"*. As the result from the running command shown value 3004, the analysis result can proceed to the next stage which is 'Read result'.

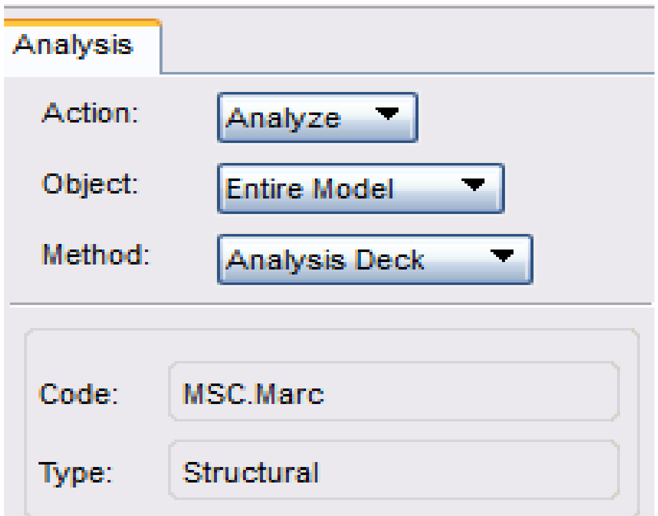

Figure 3.17: Analysis model

Figure 3.18: Command Prompt dialog box

3.4.8 Results

Select the Result tab as displayed in Figure 3.18 and Action: Create, Object: Quick Plot are choose in order to get the finalize result of the simulation. The stress, Global system is used in select Fringe Result. The displacement of translation is used for the deformation result. The von Mises criterion is selected in determines the result of the failure pressure based on the defect pattern. Figure 3.19 shows the simulation result of von Mises using quick plot. On the right side of the Figure 3.19, it shows the value of Mises stress acting on the pipe when the inner pressure applied about 120 MPa, where the highest value shows the maximum stress acting towards the pipe when the pressure is applied.

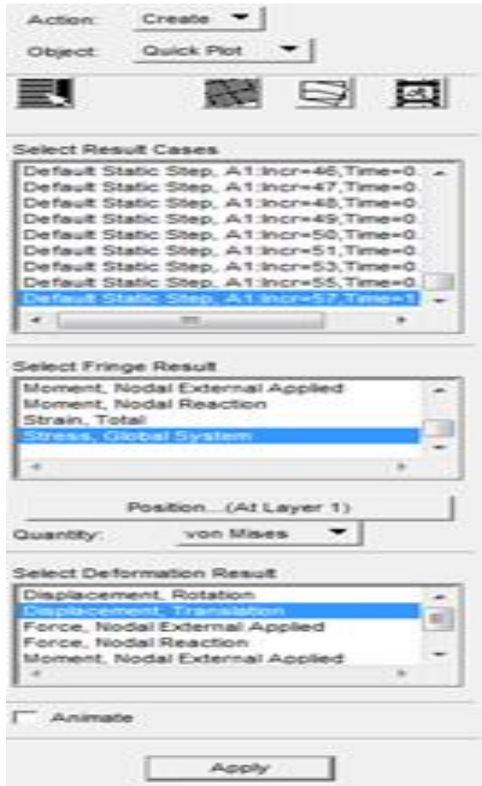

Figure 3.19: Result: Quick plot data

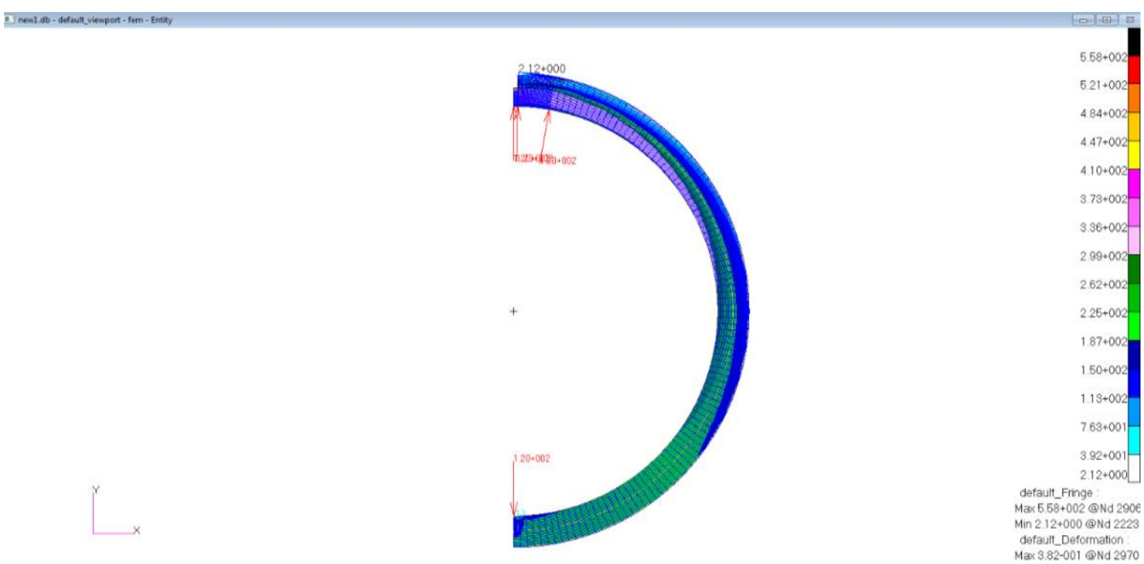

Figure 3.20: Result after simulation

3.5 DETERMINATION OF GRADE PIPE

The experimental data from spectro analysis had been done as for determining the grade B chemical composition of the steel pipe by compared with other material chemical composition. The result from experimental is shown as in Table 3.2. Based on the observation, the chemical properties for material Grade B is closed enough with the chemical composition for API 5L L245. The comparison of chemical composition based on the spectro analysis result. From the table below, API 5L L245 shows the maximum value for chemical composition. From the comparison between the grade B pipes, the values for chemical composition are nearest to the value of API 5L L245 chemical compositions.

Table 3.2: Comparison of chemical composition of material Grade B with API 5L L245 (%)

	C	**Mn**	**P**	**S**
Material Grade B	0.258	0.559	0.001	0.001
API 5L L245 (max. value)	0.26	1.20	0.003	0.003

The mechanical properties of the material Grade B is determined by using the tensile test. The data of the stress strain will be converted to the true stress strain to be used in the field section in the finite element analysis for the plastic region data. Figure 3.3 shows the graph of true stress strain from the tensile test.

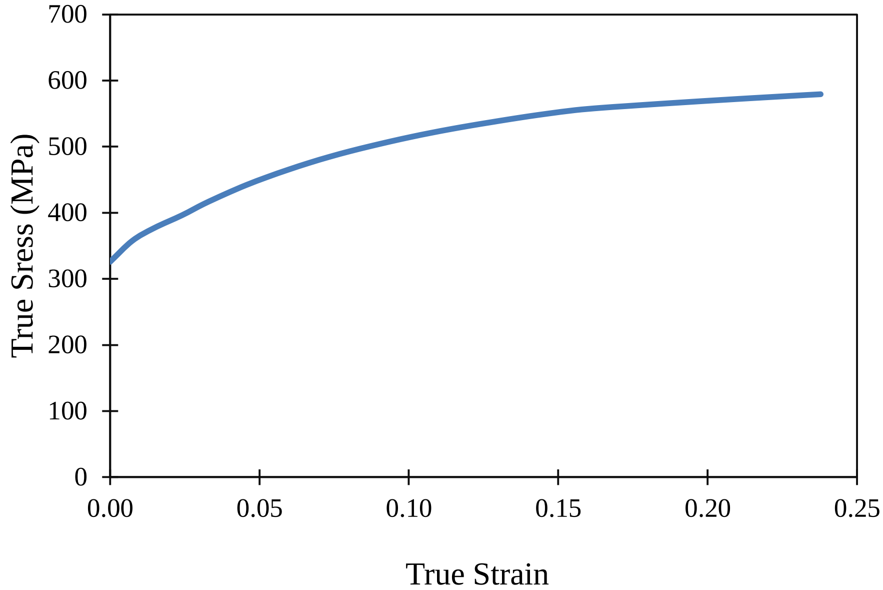

Figure 3.3: True stress strain graph from tensile test

CHAPTER 4

RESULT AND DISCUSSION

4.1 INTRODUCTION

This chapter discusses about the result obtained from the analysis of assessment on effect of geometry defect for steel pipe using finite element analysis. The objective of this research is to simulate the effect crack geometry on steel pipeline with variable defect depth and also to analyses the effect of maximum pressure on steel pipeline with variable defect geometry.

In this research, type of defects choose to be investigated are rectangular defect and groove defect. The true stress and true strain curves for the steel pipeline material API L245 is used in this FEA simulation. The FEA results are the simplest way in determining burst pressure of defective pipes based on the plastic collapse or evolving of the stress level of cross-section based on deepest point of the defect area (F. Gabor and V. Laszlo, 2011). The defect for this research is about external defect of pipeline. Depth and width of the defects are variable as being stated in Table 3.1.

During simulation, the pipe was pressurized up to 200 MPa for inner pressure. Each model been analysed, the von Mises stresses determined by FEA of inner and outer surface of steel pipe as presence of corrosion defect with variable depth. Structural FEA simulations of steel pipe were performed for the D = 60.5 mm and t = 4mm. Three different widths were simulated with lengths of 0.2, 0.5 and 1mm for every defect shape and defect depth.

4.2 STRESS DISTRIBUTION FOR DEFECT SHAPES

The experimental result is quite important in order to compare to the finite element analysis. The expected result is the pipe will be burst up at the cracks area which is the both of the cracks will interact with each other. The maximum pressure will be recorded after the pipe will burst up. The result of the two experiments is the experimental result. All the result will be discussed briefly.

Figure 4.1 and 4.2 show the comparison between defect shape (groove defect and rectangular defect) when defect depth is 50% of the thickness of pipe. The deformation of true stress strain for case 4 can be seen in Figure 4.1 and 4.2. Each of the design has its own characteristic of stress distribution. The different colors shown on the surface of the pipe corrosion defect indicated the level of the von Mises stress at each pressure applied. The simulation is to analyses the effect of defect shape, width and depth.

Figure 4.1 (a-f) shows the von Mises stress contour of the groove defect with 50% defect depth. The deformation of stress contour is developed with increasing of the internal pressure. In figure 4.1 (b), shows that the distribution of von Mises stress, start to develop at the root of the groove defect and diverges across the ligament of the pipe as the pressure rise. Stress distribution grew slowly at the pipe ligament as increase in time increment. The stress focuses more on the defect region, the maximum stress can be found at the root region of the groove defect. The growth and pattern of the stress contours can predict the burst pressure of the pipe. Based on figure 4.1 (d), when pressure achieved P= 66 MPa, the pipe predicted to fail in operation due to Mises stress exceed ultimate tensile strength of the pipe, UTS = 465MPa.

Furthermore, the patterns of von Mises stress distribution of different width are almost similar for shallow and deep defect. The stress concentration is higher at the bottom of the groove defect even the defect depth are different. The maximum stress can be determined at the middle of the groove curve. It clearly seen that, the inner surface ligament have higher stress concentration compare with the outer surface of the pipe.

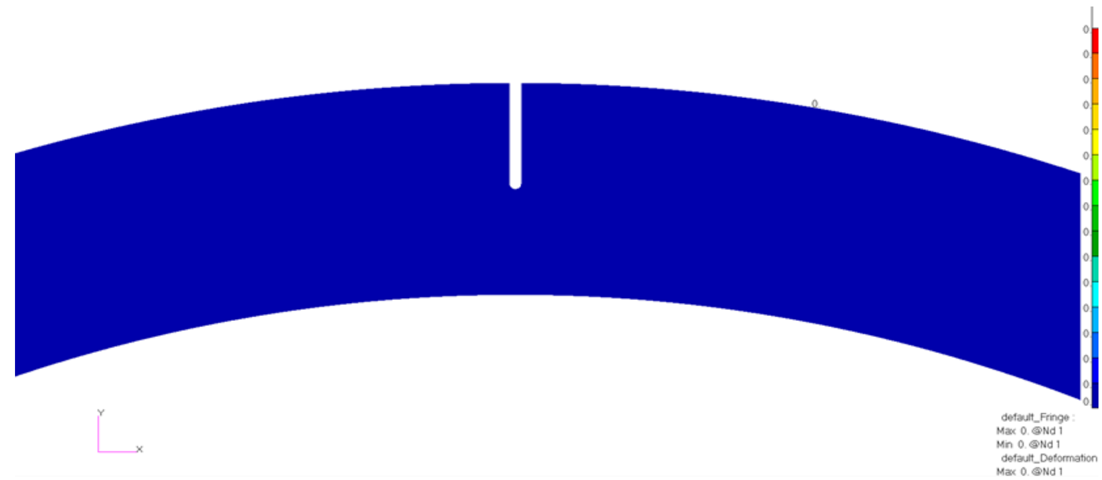

(a) P=0 MPa, Stress = 0

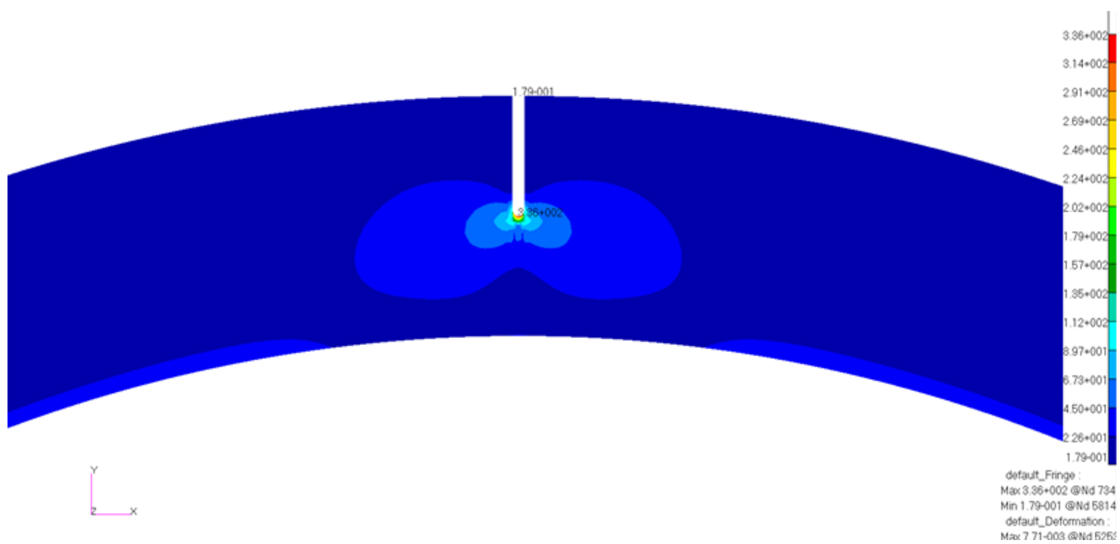

(b) P = 10MPa, Stress = 336MPa

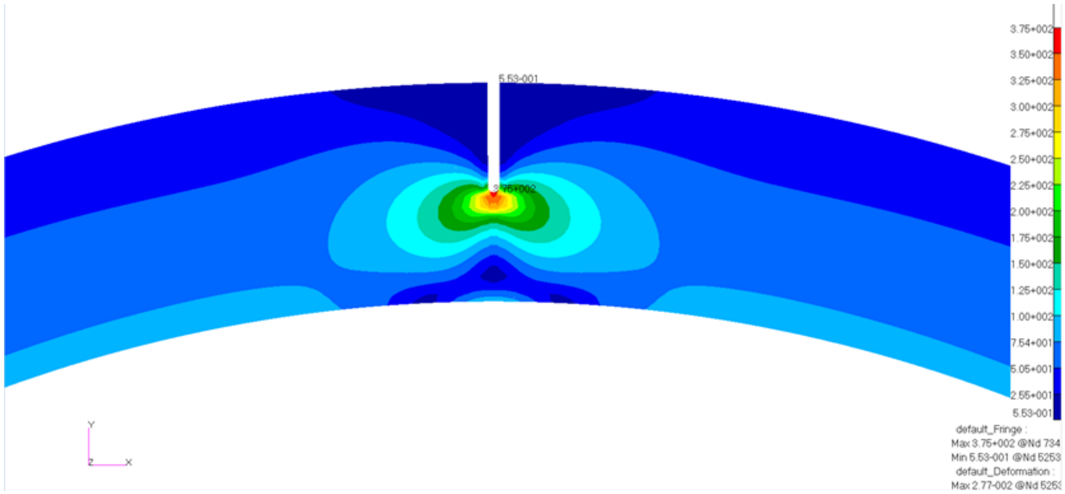

(c) P = 48MPa, Stress = 375MPa

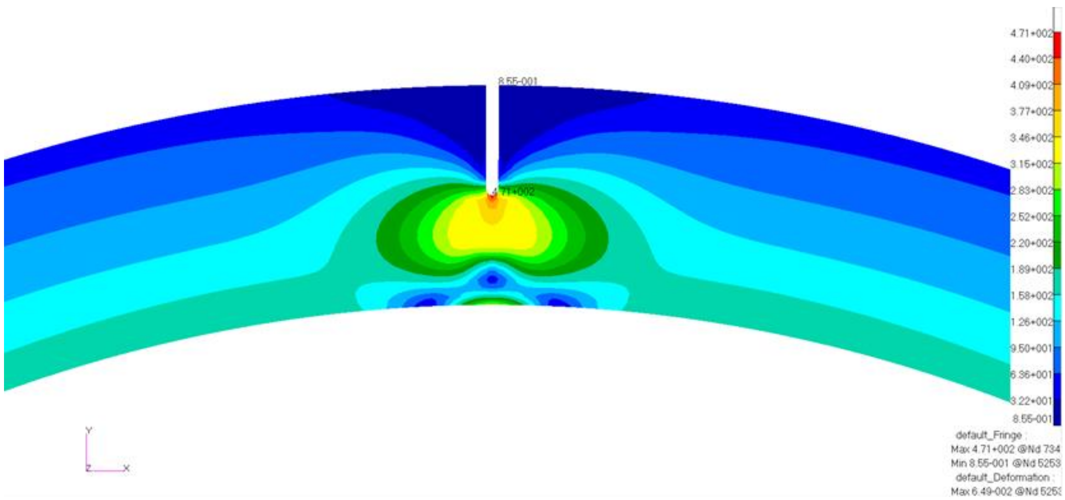

(d) P = 66MPa, Stress = 471MPa

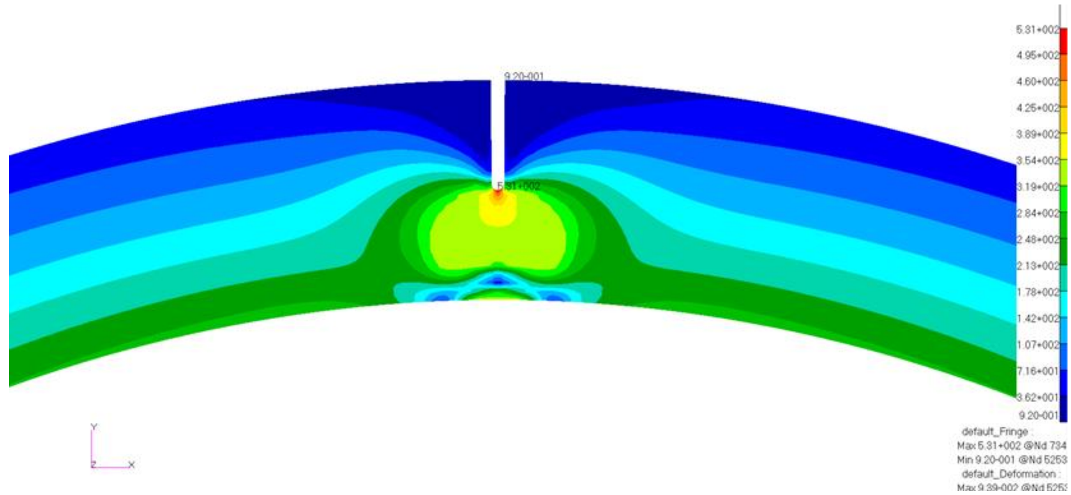

(e) P = 82MPa, Stress = 531MPa

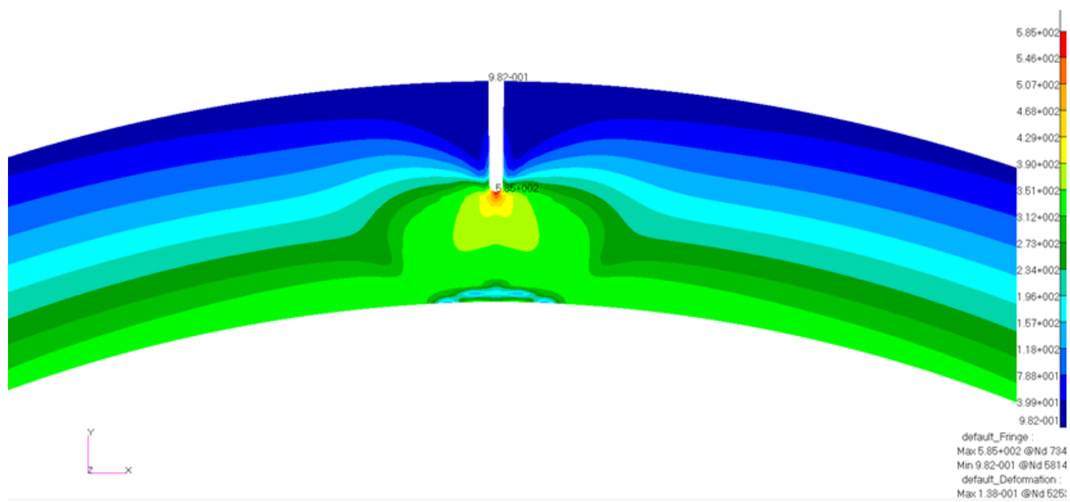

(f) P = 100MPa, Stress = 585MPa

Figure 4.1: (a-f) Von Mises stress contour for groove defect with deep defect 50%

Figure 4.2 (a-e) shows the von Mises stress distribution on pipe ligament with depth defect 50% and width defect 0.2mm. There is no stress concentration occurred during pressure 0MPa. During the pressure rise, the stress concentration of the rectangular defect spread to the pipe ligament. From the figure it is seen that a stress concentration early developed at the base of the corrosion defect. In figure 4.2 (b) the stress concentrations is about 350MPa occurred in the middle of the defect with pressure 30MPa. At a pressure of 78MPa, the von Mises stress clearly seen occurred at the edge of the rectangular defect at a stress level about 473MPa. At this state of stress concentration, the pipe assumed to be failed in operation due to it reached the value of ultimate tensile strength which is 465MPa. At time 1, the stress contours show that the stress concentration is higher at internal pipe compared to the outer surface of the pipe and most of the ligament below defect shaped achieved yield point.

During the increase of depth defect, the stress concentration will be higher on the defect curve which turns the pipe easier to be failed. Moreover, the less internal pressure reached plastic deformation as the depth defect increase.

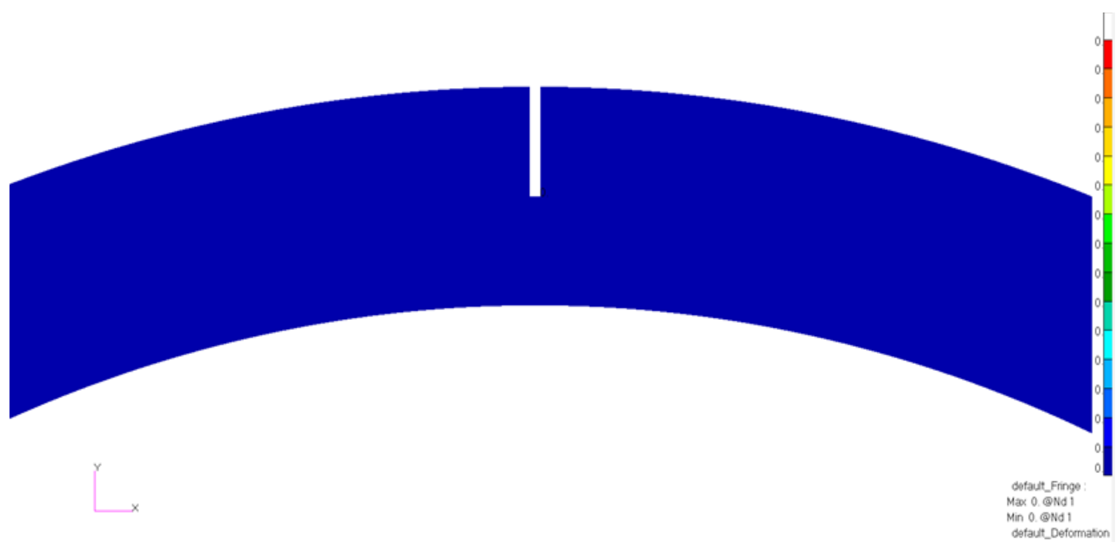

(a) P = 0MPa, Stress = 0MPa

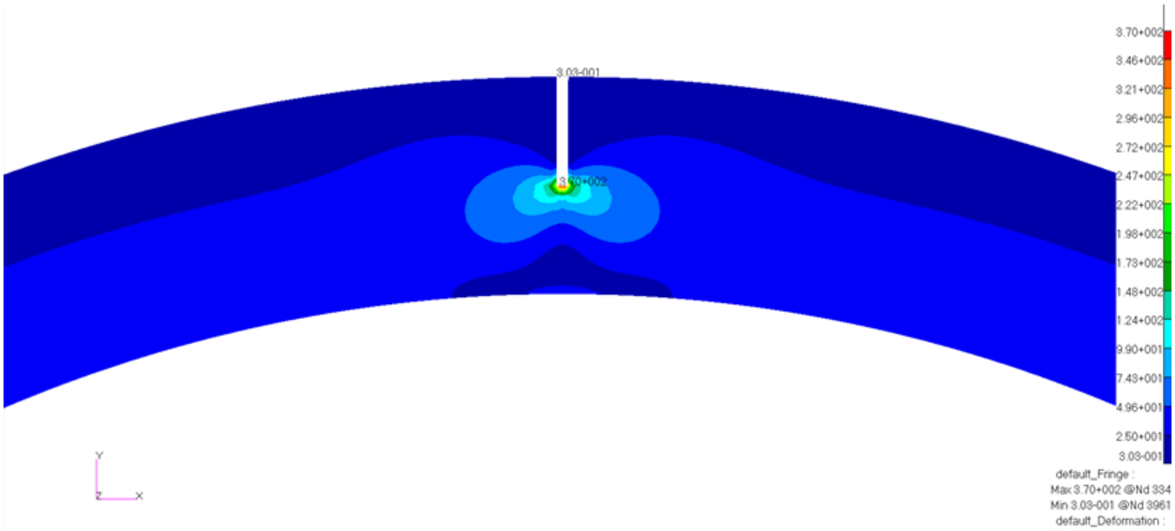

(b) P = 16MPa, Stress = 370MPa

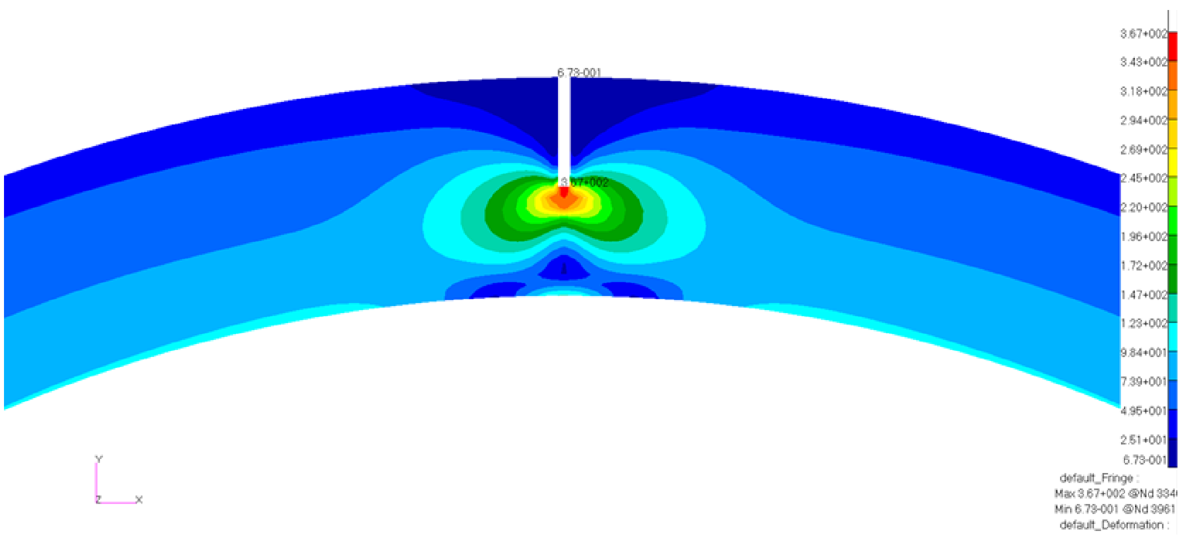

(c) P = 40MPa, Stress = 367MPa

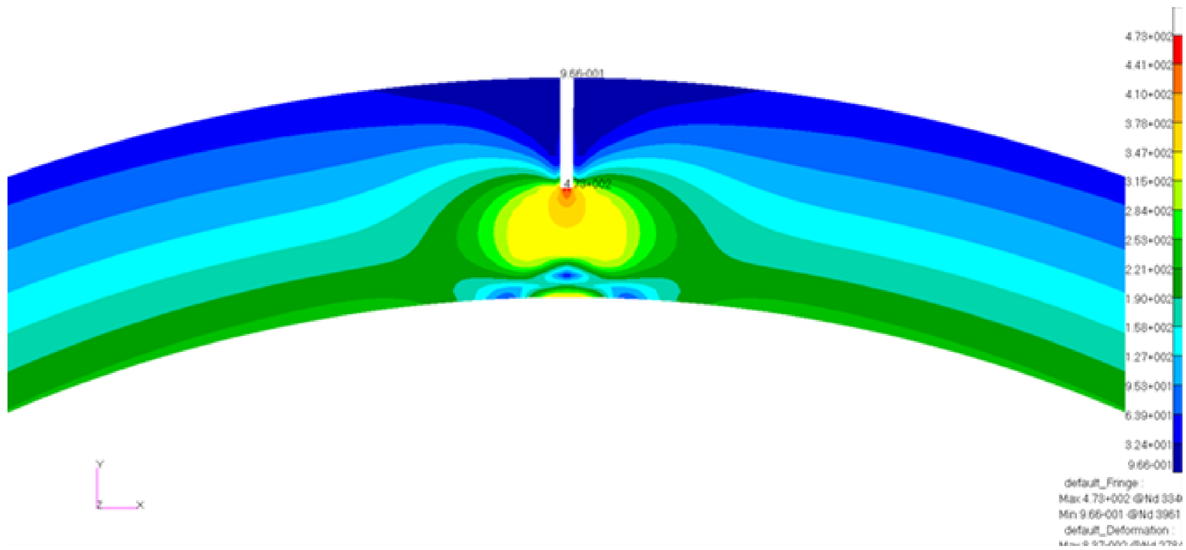

(d) P = 78MPa, Stress = 473MPa

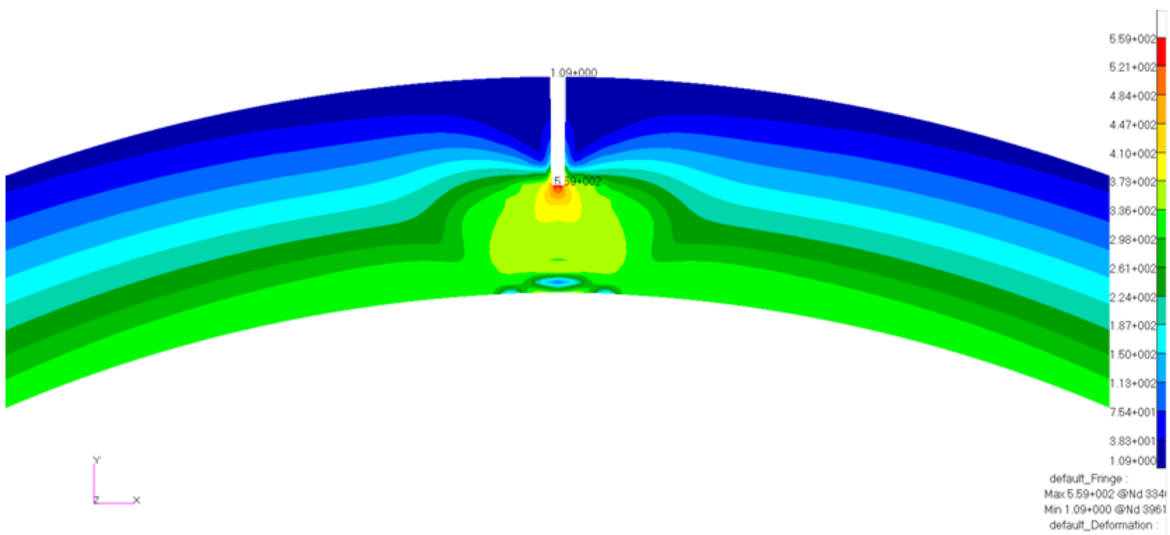

(e) P = 100MPa, Stress = 559MPa

Figure 4.2: (a-e) Von Mises stress contour for a rectangular defect with deep defect 50%

4.3 THE EFFECT OF WIDTH WITH DIFFERENT DEPTH OF DEFECT FOR RECTANGULAR AND GROOVE SHAPE BASED ON ULTIMATE TENSILE STRENGTH

The ultimate tensile strength (UTS) is a maximum stress corresponding to the maximum load applied to the material while being pulled or stretched before it breaks. It is usually performed through the tensile test by recording the stress versus strain. The ultimate tensile strength used as a guidance to predict the burst pressure of the pipeline, based on the material used for the pipe.

The tensile experiment had been performed in order to obtain the ultimate tensile strength for the material grade B. Based on the result of tensile test, the ultimate for material API 5L L245 is 465MPa. The value of the ultimate tensile strength used in taking data result from the simulation for groove and rectangular defect. The maximum stress point based on the simulation is chosen as to determine ultimate strength increment in order to get the burst pressure data. As the simulation result equal or above the limitation of UTS value, the pipe condition will considered to be failed in operation.
The main objective for this research is to simulate the effect of crack geometry on steel pipeline with variable defect depth. In order to achieve this objective, there were about 18 designs of various geometry defects and width defects. Corrosion defects were treated as rectangular and groove shape. The main goal for the simulation part is to determine how the width of corrosion defects and depth of thickness wall influence burst pressure of the pipe.

4.3.1 Ultimate tensile strength for groove defect

The failure pressure of steel pipe API 5L L245 with groove defects and various depths determined by FEA model are shown in Table 4.1 respectively. There were about three different defect widths were simulated as to investigate effect of burst pressure. The result plotted in Figure 4.3 shows that, every defects width, the burst pressure are of the steel pipe predicted by all models have small different in term of burst pressure value and the value are almost constant with increase in width defect.

The groove defect were investigated by analyzing different depth of the thickness wall defect, a = 20%, 50% and 75%, where a is the corrosion defect with fixed depth. Table 4.1 shows the tabulated data for depth of corrosion defects with variable width of groove shape defect. For case 0.2 mm width defect with different corrosion depth defect shows different values of burst pressure acting toward the pipe. From Figure 4.3, case 20% depth defect (shallow defect) the pipe failed at P_b = 144MPa. Meanwhile, in case 50% (moderately defect) and 75% (deep defect) of defect depth with width defect 0.2 mm, the burst for each case reached when P_b = 66MPa and P_b = 36MPa. The width defect pattern for d_g = 0.5 mm and 1 mm were almost the same as the width defect d_g = 0.2 mm, where the deep defect show lower burst pressure compare to the shallow and moderately defect. As expected, the deeper defects fail at lower failure pressures compare to the moderately deep defect (50%) and shallow defects (20%).

Table 4.1: Depth of corrosion defects with variable width of groove shape defect

Defect width, d_g (mm)	**Burst Pressure, P_b (MPa)**		
Depth Defect (%)	**20**	**50**	**75**
0.2	144	66	36
0.5	153.6	80	48
1	165.6	96	54

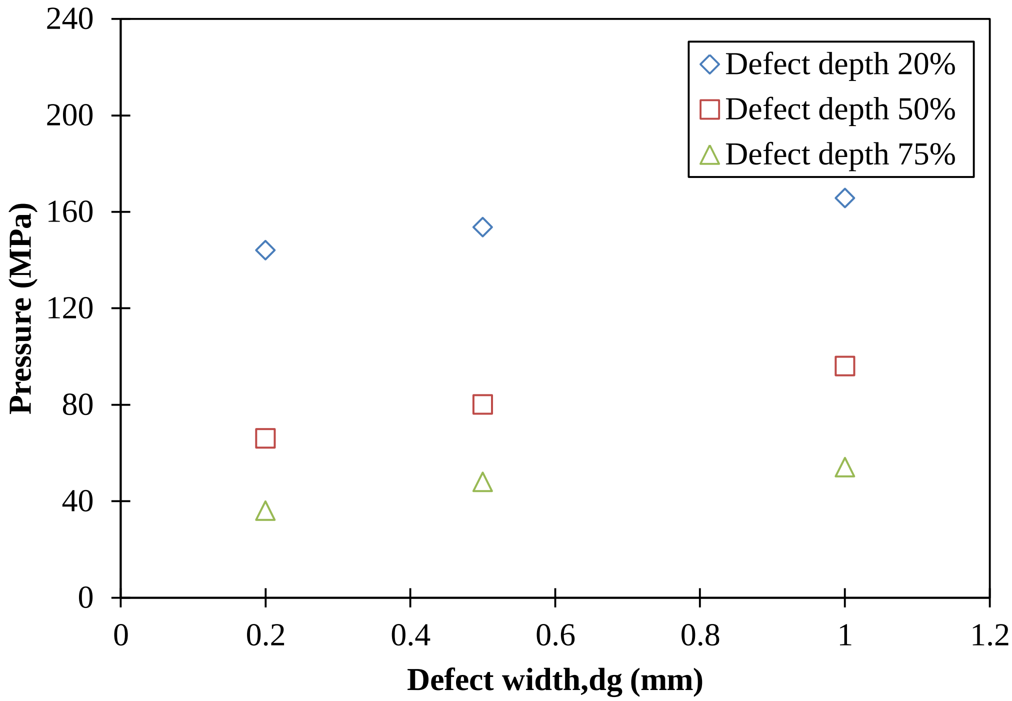

Figure 4.3: Burst pressure of different depth steel pipe as a function of variable width of groove corrosion defect

Table 4.2, shows detail value for the comparison between industries codes with FEA result of groove defect for ultimate tensile strength determined by FEA model. Based on figure 4.4, it shows the comparison between the ultimate tensile strength of FEA analysis with the industry codes. The UTS value is selected based on maximum point of the defect curve. The burst pressure obtained from FEA result is much greater than industry codes. The highest value of burst pressure is obtained by width defect 1mm, P_b = 165.6MPa. Meanwhile, the lowest value of burst pressure is obtained at P_b = 36MPa with width defect of 0.2mm. The burst pressure will be lower when increase in depth of defect.

Table 4.2: Comparison between industries codes with FEA result of groove defect for ultimate tensile strength

	Burst Pressure, P_b (MPa)					
Corrosion Defect(%)	ASME B31G	Modified ASME	DNV-RP-F101	dg 0.2mm	dg 0.5mm	dg 1mm
20	37.93	43.01	55.66	144	153.6	165.6
50	23.71	27.79	38.03	66	80	96
75	11.85	13.61	20.62	36	48	54

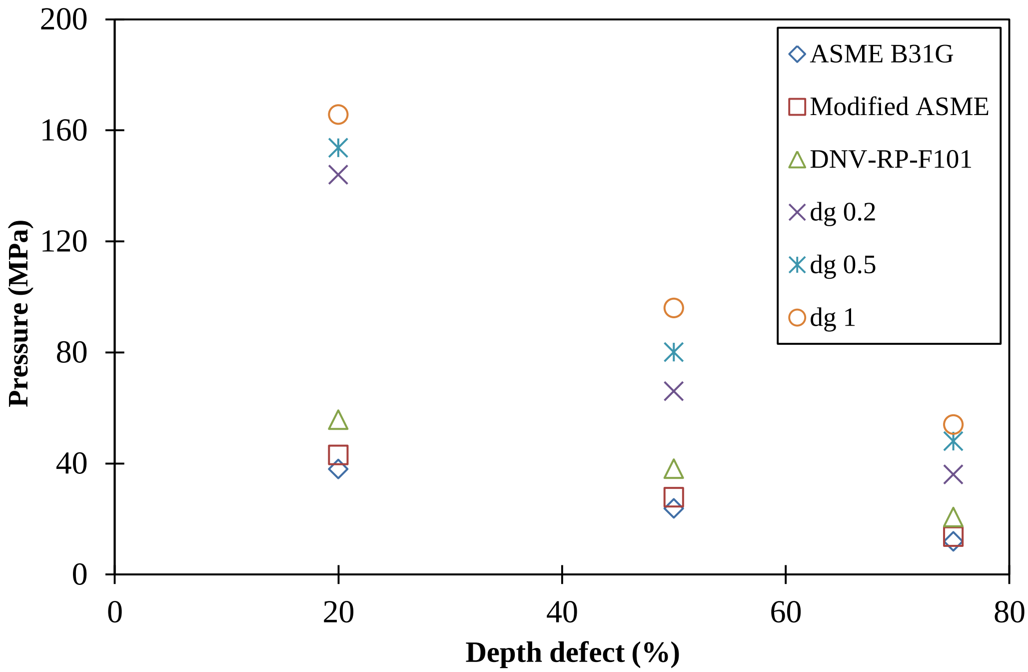

Figure 4.4: Ultimate strength of groove defect

4.3.2 Ultimate strength for rectangular defect

Figure 4.5 shows the burst pressure determined by FEA for rectangular shape defect with variable in width of defect. Meanwhile, in Table 4.3, it shows the value for depth of corrosion defects with variable width of rectangular shape defect. As expected, there are small different in burst pressure for variable width defect. The value for each depth defect with various width defect size have small differences to each other. For example depth defect of 75%, the P_b for 0.2 mm, 0.5 mm and 1 mm width defect are 44.4MPa, 52.8MPa and 56.4MPa each. It clearly shows that, the width does not affect much to the burst pressure value.

However, in terms of depth defect, the shallow defect, 20% depth defect has higher value of burst pressure compare to the moderately defect, 50% and deep defect, 75% of wall thickness. Based on the result of simulation, the burst pressure can be considered to be the same for width defect, but for the defect depths were different. Based on these result, it can be conclude again that the deep defect cannot withstand high pressure compare to the shallow defect and moderately. The pipe operation may fail early for deep corrosion defect.

Table 4.3: Depth of corrosion defects with variable width of rectangular shape defect

Defect Width, w_c (mm)	**Burst Pressure, P_b (MPa)**		
Corrosion Defect (%)	**20**	**50**	**75**
0.2	154.8	76	44.4
0.5	168	88	52.8
1	172	99	56.4

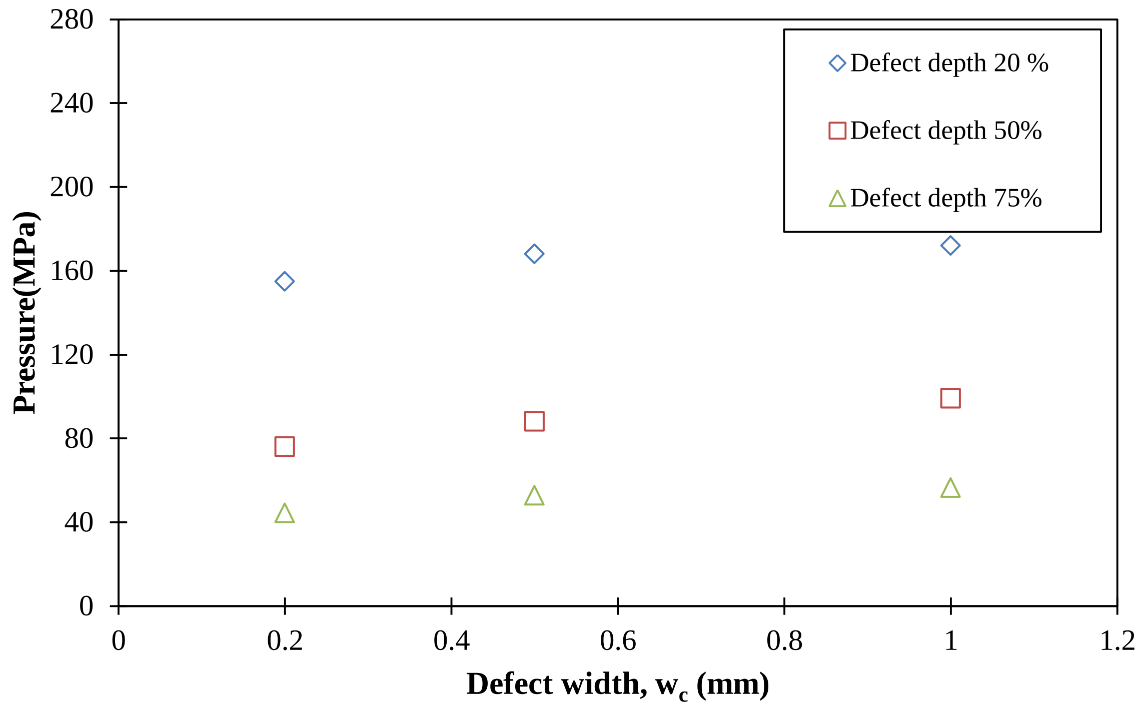

Figure 4.5: Burst pressure of different depth steel pipe as a function of variable width of rectangular corrosion defect

Based on Figure 4.6, it shows the comparison result of FEA ultimate tensile strength with industry codes. As expected, the result from FEA is higher compare to the calculated codes. The value from industry codes calculation is compared with the analysis value in order to estimate the burst pressure of the pipe. Based on the result, the width defect 1mm with 20% defect depth has higher value of burst pressure, P_b = 172MPa compared to the value of 0.5mm and 0.2mm width. The small value of burst pressure, P_b = 44.4MPa, occurred at defect width 0.2mm with depth 50% of wall thickness. The burst pressures for 0.2 mm of width are much closed to the DNV-RP-F101 compared to other codes such as ASME B31G and Modified ASME. In Table 4.4, shows detail about the value of comparison between industries codes with FEA result of rectangular defect for ultimate tensile strength from FEA model.

Table 4.4: Comparison between industries codes with FEA result of rectangular defect for ultimate tensile strength

	Burst Pressure, P_b (MPa)					
Corrosion Defect(%)	**ASME B31G**	**Modified ASME**	**DNV-RP-F101**	**w_c 0.2mm**	**w_c 0.5mm**	**w_c 1mm**
20	37.93	43.01	55.66	154.8	168	172
50	23.71	27.79	38.03	76	88	99
75	11.85	13.61	20.62	44.4	52.8	56.4

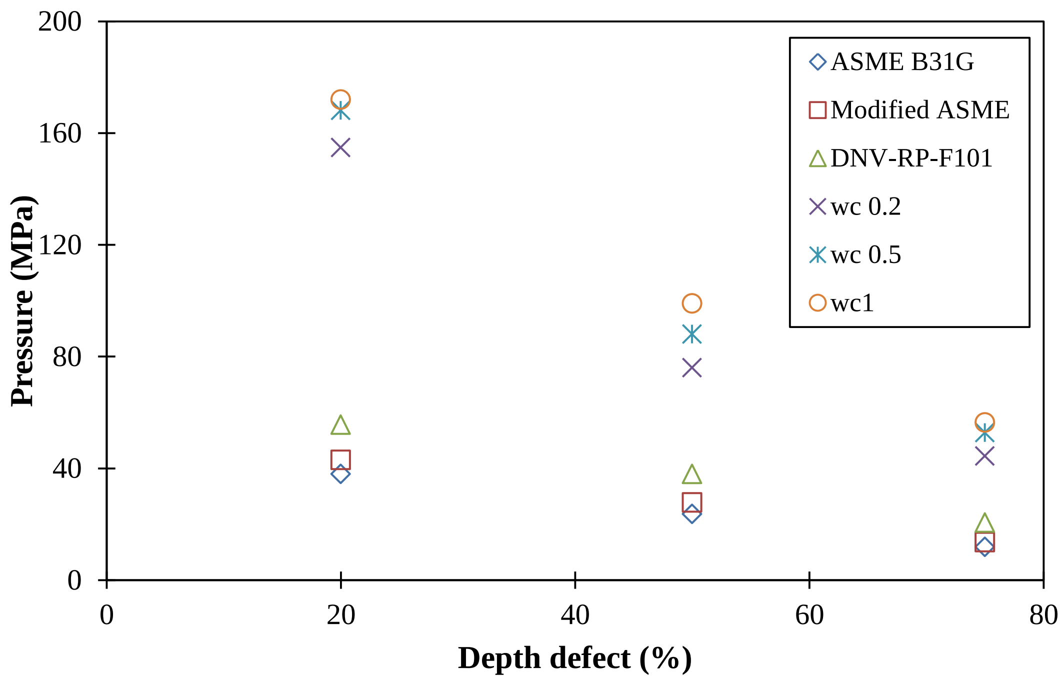

Figure 4.6: Ultimate strength of rectangular defect

4.3.3 Effect of depth on the width geometry defect.

In Figure 4.7, shows the comparison of burst pressure between groove and rectangular defect based on width size 0.2 mm. Besides, in Table 4.5, the values of the depth defect with 0.2 mm width defect are included. It is clearly seen that, the groove defect is easy to fail in operation rather than rectangular due to the lower burst pressure of the pipe simulation.

The percent different for groove and rectangular defect 20% depth defect is about 7.5%. Meanwhile, for 50% and 75% depth defect, the percent different between groove and rectangular defect are 15.2% and 23.3%.

Table 4.5: Depth defect with 0.2 mm width defect

	Burst Pressure, P_b (MPa)		
Depth Defect (%)	**20**	**50**	**75**
Groove	144	66	36
Rectangular	154.8	76	44.4

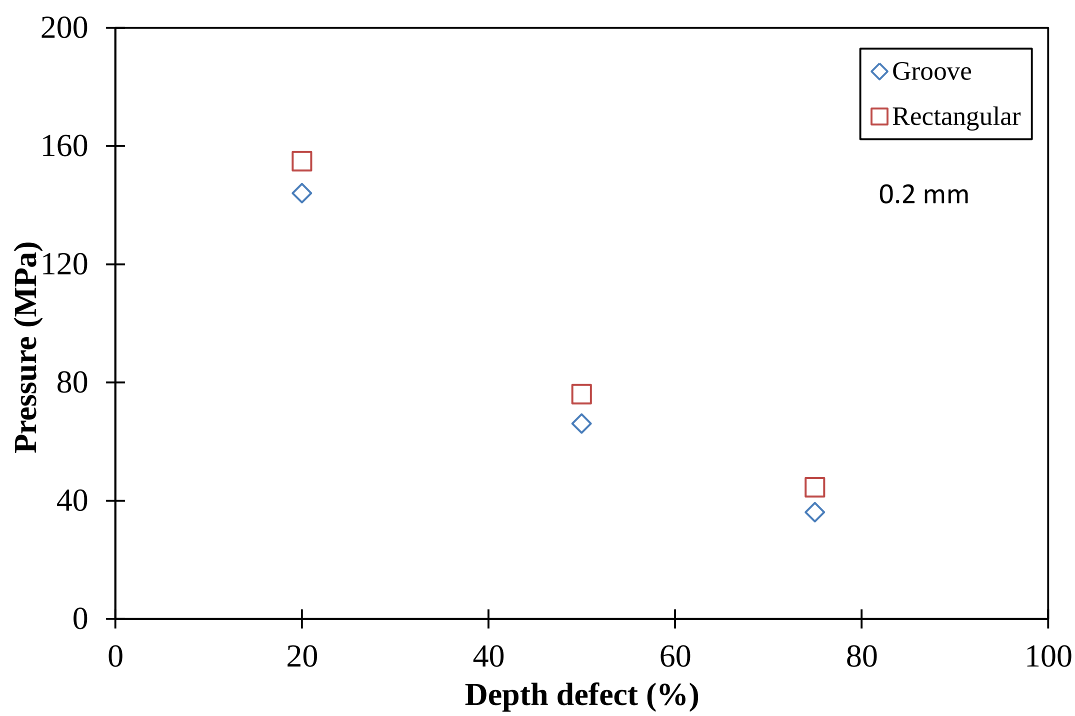

Figure 4.7: Burst pressure based on the width defect 0.2 mm

Based on Figure 4.8, the depth defect with width defect 0.5 mm have similar pattern with width defect 0.2 mm, where the groove defect have lower value of burst pressure.

The percent different between groove and rectangular defect for 20%, 50% and 75% defect depth are 9.37%, 10% and 10%. Table 4.6, shows detail value for defect depth with 0.5mm width defect.

Table 4.6: Depth defect with 0.5 mm width defect

	Burst Pressure, P_b (MPa)		
Depth Defect (%)	**20**	**50**	**75**
Groove	153.6	80	48
Rectangular	168	88	52.8

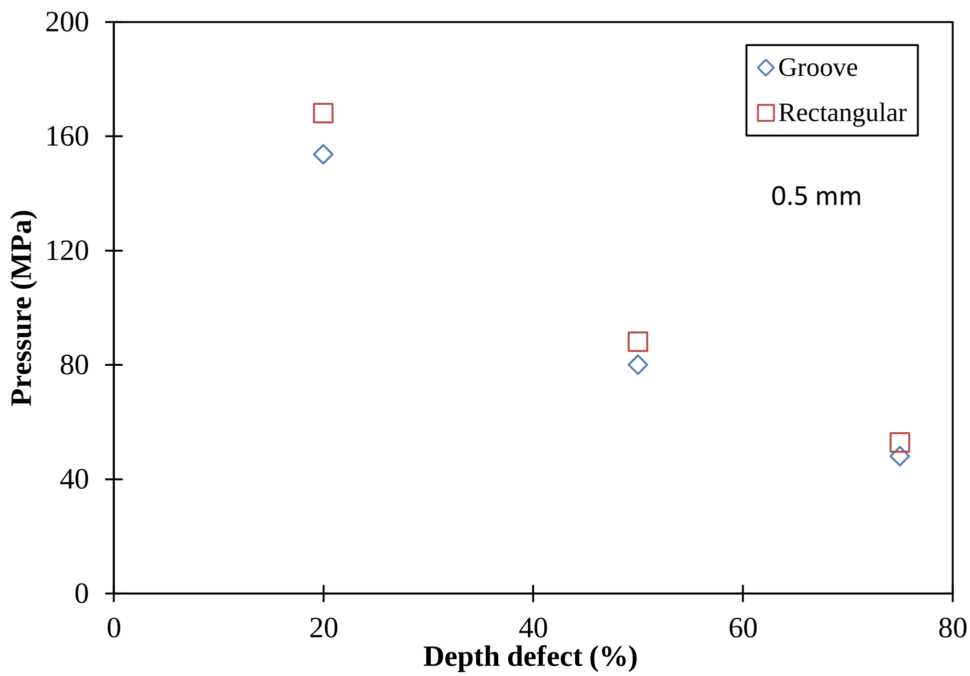

Figure 4.8: Burst pressure based on the width defect 0.5 mm

Figure 4.9 shows, the depth defect with width defect of 1 mm. The percent different groove and rectangular defect for 20%, 50% and 75% defect depth are 3.8%, 3.1% and 4.4%. Table 4.7 shows the detail value for depth defect with 1 mm width defect based on the FEA model.

Table 4.7: Depth defect with 1 mm width defect

	Burst Pressure, P_b (MPa)		
Depth defect (%)	**20**	**50**	**75**
Groove	165.6	96	54
Rectangular	172	99	56.4

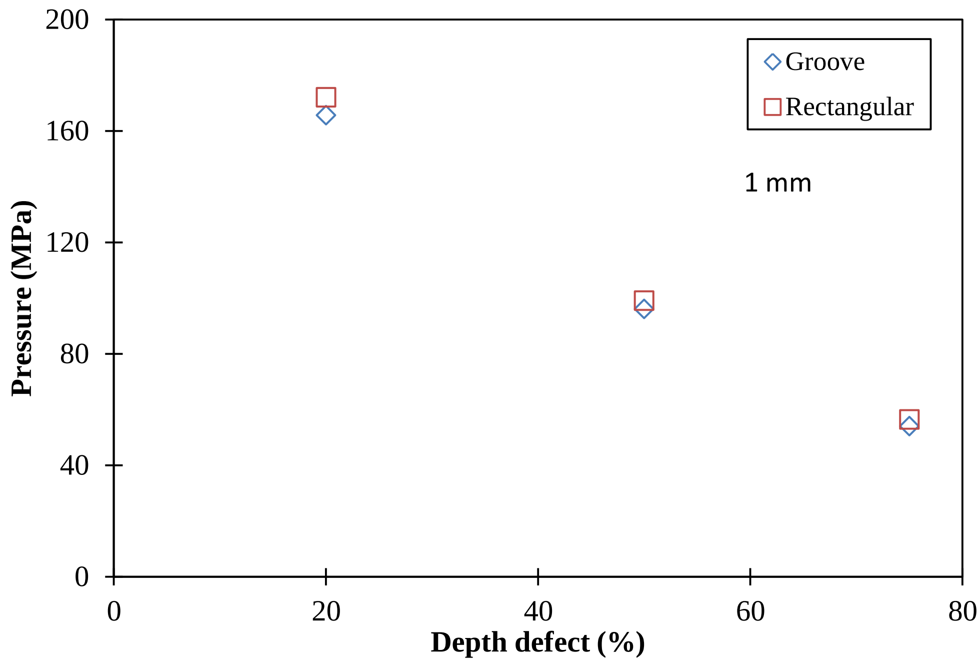

Figure 4.9: Burst pressure based on the width defect 1 mm

4.4 THE EFFECT OF WIDTH WITH DIFFERENT DEPTH OF DEFECT FOR RECTANGULAR AND GROOVE SHAPE BASED ON TENSILE STRENGTH

The yield strength (YS) is stress which corresponding to the pressure applied to the material during tensile test. The yield strength is a predetermined amount of permanent deformation to be occurring. It is usually performed through the tensile test by recording the stress versus strain. Yield strength is a stress of material which start to deform plastically.

Based on the stress-strain curve, the YS for material API 5L L245 is determined to be 326MPa. The maximum stress point of simulation is choose as to get the time increment for YS in order to predict early burst pressure of the pipe.

4.4.1 Yield strength for groove and rectangular shape of defect geometry

According to Figure 4.10, shows the pressure achieved based on yield strength of groove defect with variable depth and width defect. From the result, it shows that, the width 0.2mm has lower burst pressure compare to the width of 0.5mm and 1 mm referred to depth defect 20%. Besides, at depth 50% and 75%, the widths 0.5 mm have higher of pressure, P_b rather than 0.2mm and 1mm. However, the deep defect still easy to achieve burst pressure compare to the shallow defect.

Table 4.8: Depth of corrosion defects with variable width of groove shape defect

Defect width, d_g (mm)	**Burst Pressure, P_b (MPa)**		
Depth of defect (%)	**20**	**50**	**75**
0.2	25.6	10	4.8
0.5	144	70	40.8
1	162	18	8.4

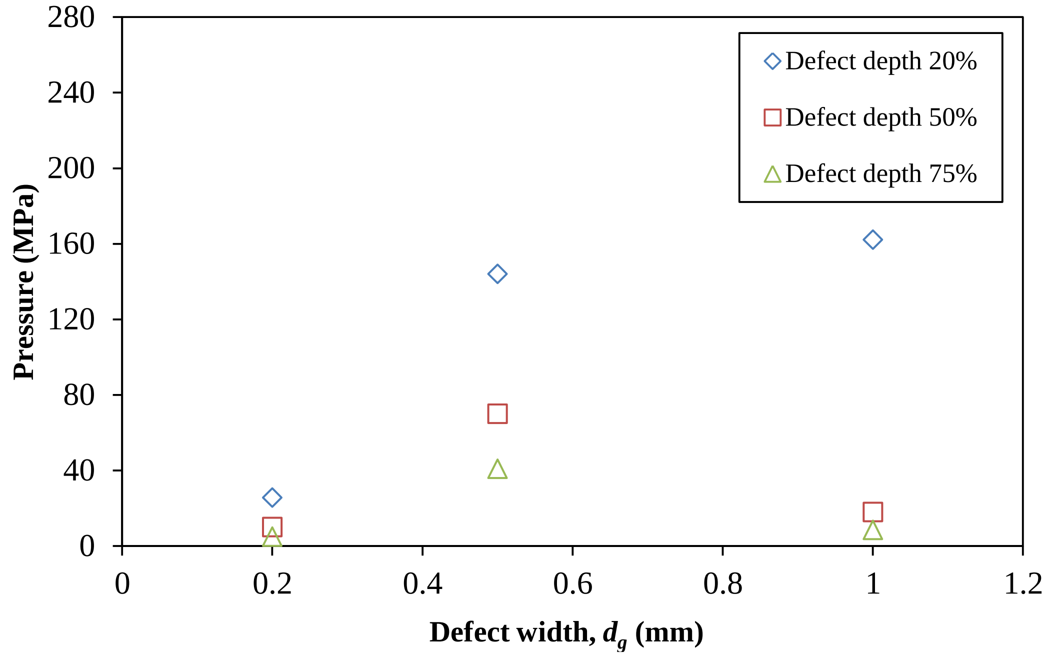

Figure 4.10: Burst pressure of different depth steel pipe as a function of variable width of groove corrosion defect

From Figure 4.11, the result shows the burst pressure of rectangular defect with variable width of defect. As expected that, the width defect does not affect much in burst pressure rather than the depth defect. The higher value of burst pressure is when the depth is 20% followed by 50% and 75% of depth defect. The burst pressure for each width size shows the result are almost constant due to the small different between width defect. Table 4.9 shows detail about the value of the depth of corrosion defects with variable width of rectangular shape defect based on the FEA model.

Table 4.9: Depth of corrosion defects with variable width of rectangular shape defect

Defect width, w_c (mm)	**Burst Pressure, P_b (MPa)**		
Depth defects (%)	**20%**	**50%**	**75%**
0.2	154.8	76	44.4
0.5	168	88	52.8
1	172	99	56.4

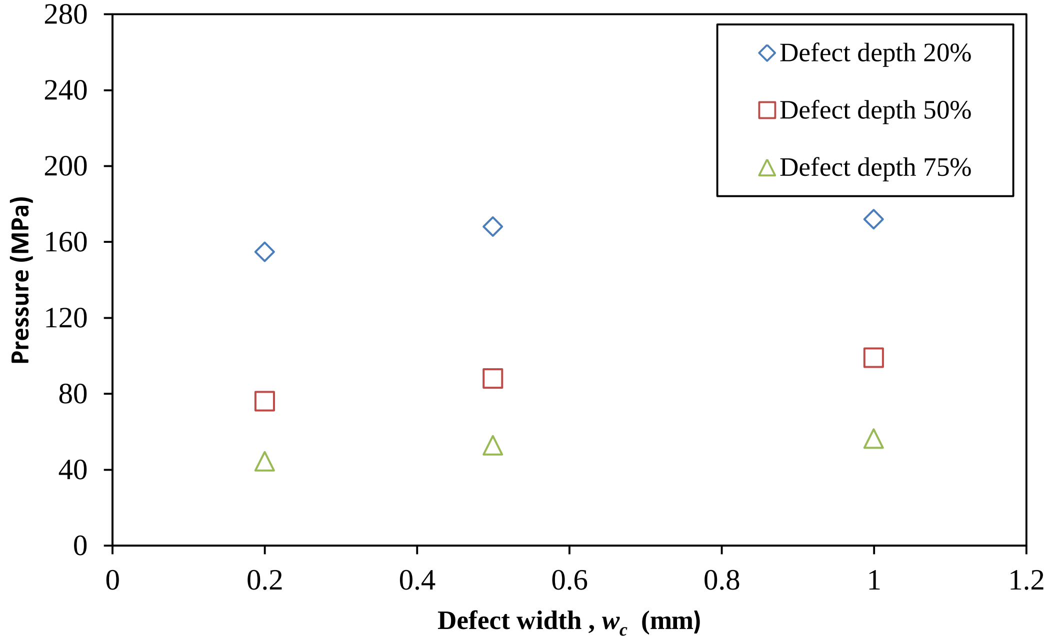

Figure 4.11: Burst pressure of different depth steel pipe as a function of variable width of rectangular corrosion defect

4.4.2 Comparison of industry codes with FEA result based on yield strength

Figure 4.12 shows the pressure of steel grade B with groove corrosion defect with various depth defect determined by industry codes and FEA model based on the average yield strength, respectively. It is seen that the groove defect with width of 0.2 mm located lower than the industry codes value. The pressure reach yield point faster compared to industry codes and other FEA results (0.5mm and 1mm). At width defect 0.5 mm, the value for burst pressure of 50% and 75% are located below the industry codes, where else for depth 20%, the value for burst pressure based on yield is exceed 160MPa. Furthermore, the value for width defect 0.5mm is above the industry codes. In Table 4.10, shows detail about the burst pressure based on the industry codes and FEA model for groove defect.

Table 4.10: Burst pressure based on the industry codes and FEA model for groove defect

	Burst Pressure, P_b (MPa)					
Corrosion Defect (%)	**ASME B31G**	**Modified ASME**	**DNV-RP-F101**	**dg 0.2**	**dg 0.5**	**dg 1**
20	37.93	43.01	55.66	25.6	144	162
50	23.71	27.79	38.03	10	70	18
75	11.85	13.61	20.62	4.8	40.8	8.4

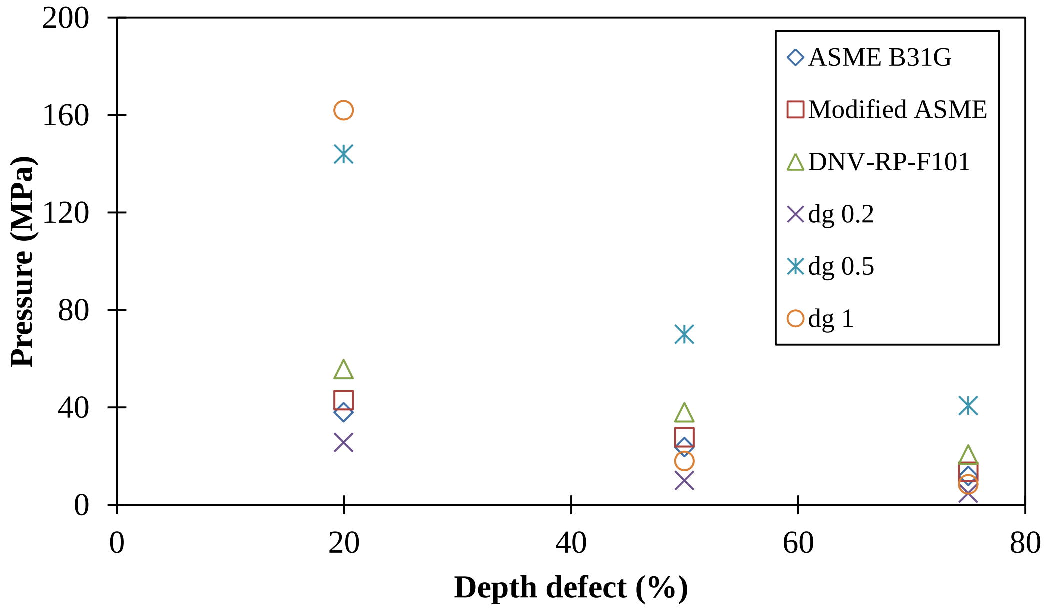

Figure 4.12: Industry codes and FEA result for groove defect

From Figure 4.13, the result shows the comparison of rectangular defect between depth defect and burst pressure based on yield strength. As expected the width defect 0.2 mm has lower burst pressure. Besides, the value of yield for depth 20% width defect of 0.5mm and 1mm are highest which about 60MPa and 76MPa for each width size. Meanwhile, for the depth 50% and 75%, each of value for width defect is located under the industry codes. The value of yield strength from FEA is closer to the industry codes ASME B31G and Modified B31G, due to the calculation for both model are used YS .

However for the DNV-RP-F101, the calculation involved of UTS value. Table 4.11, include detail about the burst pressure based on the industry codes and FEA model for rectangular defect.

Table 4.11: Burst pressure based on the industry codes and FEA model for rectangular defect.

	Burst Pressure, P_b (MPa)					
Corrosion Defect(%)	**ASME B31G**	**Modified ASME**	**DNV-RP-F101**	w_c **0.2**	w_c **0.5**	w_c **1**
20	37.93	43.01	55.66	36	60	76
50	23.71	27.79	38.03	16	18	22
75	11.85	13.61	20.62	7.2	8.4	13.4

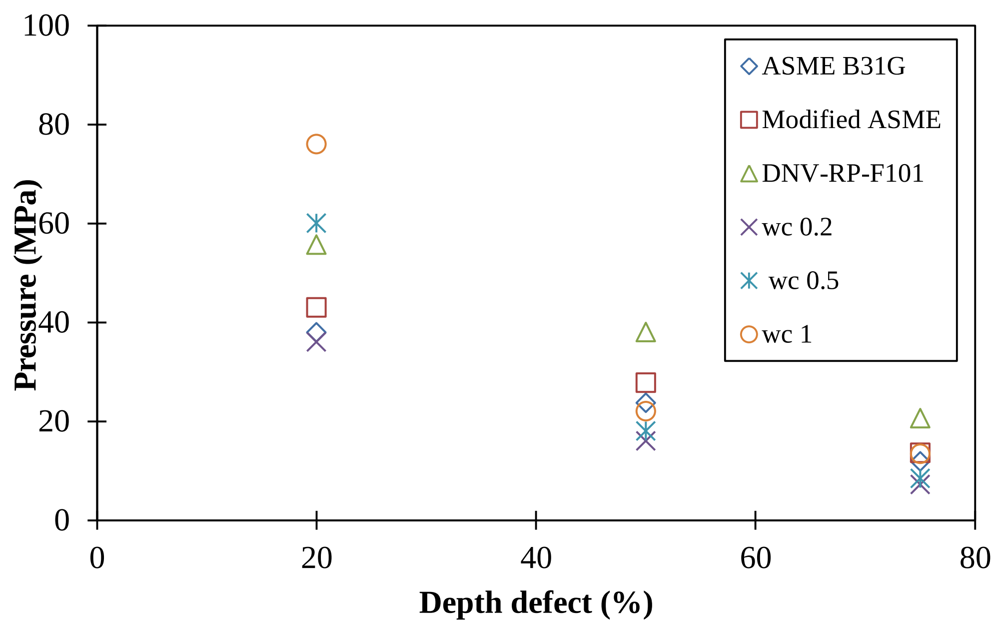

Figure 4.13: Industry codes and FEA result for rectangular defect

4.5 THE EFFECT OF WIDTH WITH DIFFERENT DEPTH OF DEFECT FOR RECTANGULAR AND GROOVE SHAPE BASED AVERAGE YIELD STRENGTH

The average of yield strength is taken through the selection of the nodes at every node along the curve defect. The selection of every node will be dividing in order to get average value of yield strength, which is 326MPa. This is to define at which level of pressure the pipe reach the yield point. The procedure to take average yield strength is the same for two type of defect geometry (groove and rectangular defect).

4.5.1 Comparison industry codes with FEA result

Based on figure 4.10, it shows the average yield strength of for groove defect. The maximum burst pressure is at 20% defect depth with 1mm width defect P_b = 158.4MPa. While the minimum value for burst pressure is at 75% with 0.2mm width defect, P_b = 24MPa.

The value of groove defect is much higher compare to the rectangular defect due to the selection of point at the curve surface. The different shape of defect may have different stress concentration at every point along the defect shape. Table 4.12, described detail on the value of comparison between industries codes with FEA result for groove defect for average yield strength.

Table 4.12: Comparison between industries codes with FEA result for groove defect for average yield strength

Corrosion Defect (%)	**ASME B31G**	**Modified ASME**	**DNV-RP-F101**	**d_g 0.2**	**d_g 0.5**	**d_g 1**
20	37.93	43.01	55.66	118.4	151.2	158.4
50	23.71	27.79	38.03	48	64	88
75	11.85	13.61	20.62	24	45.6	51.6

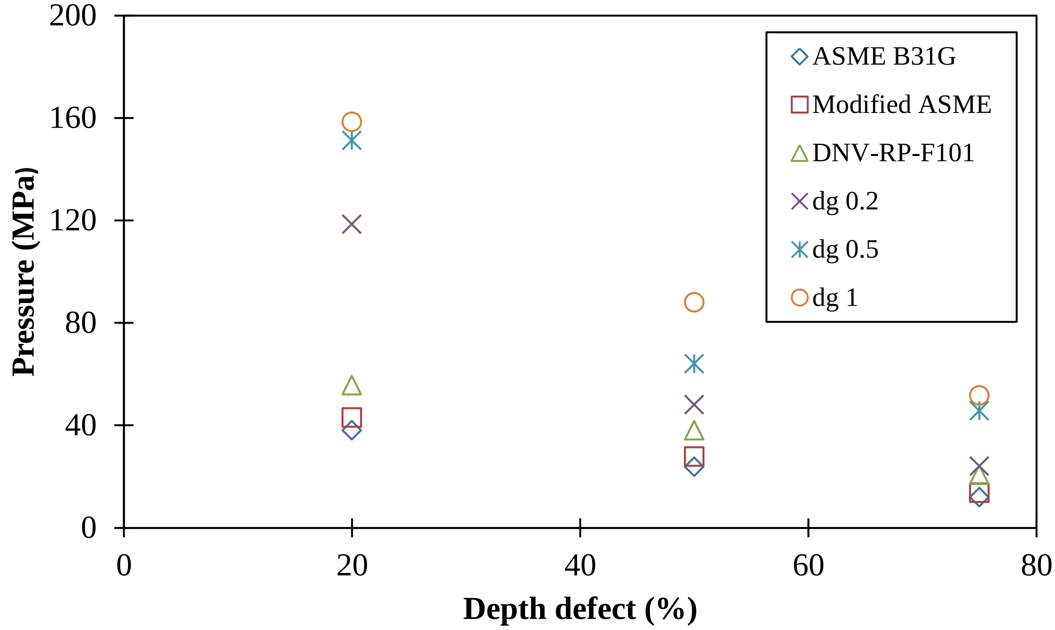

Figure 4.14.: Groove defect based on average yield stress

The figure 4.11 displayed about the comparison between industry codes and analysis data of average yield strength for rectangular defect. The codes are decrease with increase of the defect depth, same goes to the finite element analysis result. It clearly seen, the FEA results are much higher compare to the codes values ASME B31G, Modified ASME and DNV-RP-101. It shows that, the FEA result closed to the DNV–RP-101 codes which make the result for FEA is more reliable due to the result closed to the DNV–RP-F101 model. In figure above, we can see that the depths of defect are clearly influence the burst pressure of the pipe. The value defect 75% from depth shows the burst pressure below DNV-RP-F101 result for width 0.2mm, 0.5mm and 1mm. Besides, the value for width 0.2mm and 0.5mm at 50% defect show the result below to the DNV-RP-F101 code. Table 4.13, shows the comparison between industries codes with FEA result for rectangular defect for average yield strength.

Table 4.13: Comparison between industries codes with FEA result for rectangular defect for average yield strength

Corrosion Defect (%)	ASME B31G	Modified ASME	DNV-RP-F101	w_c 0.2	w_c 0.5	w_c 1
20	37.93	43.01	55.66	72	76	92
50	23.71	27.79	38.03	34	36	41.8
75	11.85	13.61	20.62	14.4	15.6	18

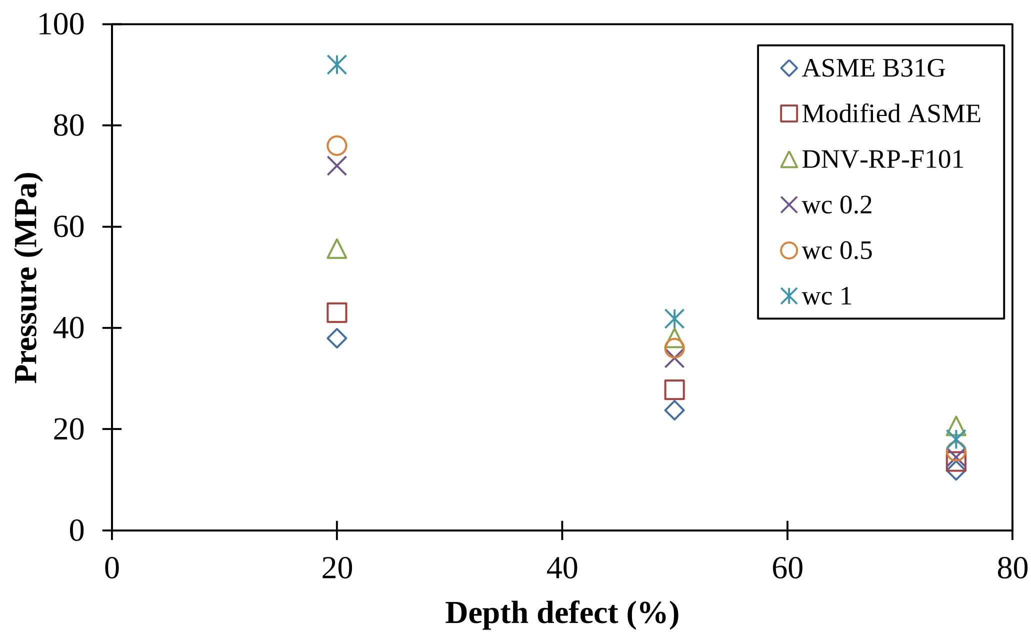

Figure 4.15: Rectangular defect based on average yield strength

4.6 DISCUSSION

4.6.1 Effect of geometry corrosion defect on the stress-strain distribution to the pipe

The geometry corrosion defect play an important affect in determined the burst pressure due to distribution of stress and strain in pipeline. Basically, the stress on von Mises is higher during the absence of the corrosion defect on the pipeline. FEA provides an easy way to calculate the stress and strain distribution on the pipe ligament. As the width of the defect increase, the von Mises stress based on UTS value are almost constant. When the depth defect is moderately as shown in Figure 4.1 and 4.2, the von Mises stress at internal surface of pipe are lower rather than at defect base for different geometry defect. With increase in terms of depth corrosion defect, it will enhance the stress concentration at the pipeline. During increasing of depth defect, it influences the von Mises stress of internal surface pipe where high stress field is distributed at in and defect region.

4.6.2 Ultimate tensile strength

The ultimate tensile strength value is determined through tensile test and recording from stress-strain graph from experimental. The highest value of stress-strain curve is known as ultimate tensile strength. It is the maximum value for the material can withstand before it being failed. The UTS value is guided to determine the burst pressure of pipeline. As the Mises stress is over limit of UTS, the material will considered to be fail in operation.

4.6.3 Prediction of burst pressure with assessment of industry codes and FEA model.

Based on the analysis in the presence work, the industry and FEA models used to predict the burst pressure of the pipeline. The depth of defect on pipe will give lower burst pressure, as it can be assume to be easily failed. The codes predict early burst pressure rather than FEA model. The shallow depth defect can withstand high pressure; it tends to reduce time for the plastic deformation to occur rather than deep defect.

From the comparison between industry models and FEA with ultimate strength, it shows that, the FEA result is close to the DNV-RP-F101 model. That make the DNV-RP-F101 become high accuracy of the burst pressure prediction among the industry codes.

4.7 SUMMARY

From this analysis, it can be concluded that the width effect have less affected in prediction of burst pressure compared to the defect depth. The burst pressure increased with decreasing of defect depth, and these results were compared with the industry codes to validate the FEA model and failure criterion. The groove and rectangular defect models have different values of burst pressure.

Based on the simulation, the groove and rectangular shape have their own behavior of von Mises stress. The stress concentration for both defect shapes start to develop at the base of the defect. The groove shape stress behaviors shown in Figure 4.1 start to developed the stress region at the root of the groove defect and diverge to entire ligament of the pipe. Meanwhile, for the rectangular defect, the stress concentrations start occurred at the edge of the defect.

Regarding the overall result shows that, different width of defect does not influence much on the burst pressure value. The deep defect will have lower burst pressure compare to the moderately and shallow defect. Based on the simulation, the burst pressure of the pipe determined when the von Mises stress on the defect pipe ligament reached the ultimate strength of the material, 465MPa, expressed as a true stress. The model will be considered to fail due to the plastic collapse. From ultimate tensile strength result, every length of the width groove and rectangular defect have almost similar pressure failure with percent different about 3% to 10%. It can be conclude that, the type of geometry defect and width defect does not influence much the burst pressure.

CHAPTER 5

CONCLUSION AND RECOMMENDATION

5.1 INTRODUCTION

This chapter will conclude the analysis research and briefly discuss about the recommendation that can conducted for future work. The conclusion were based on the result obtain in Chapter 4. In order to study the assessment on effect of geometry defect for steel pipe, other aspects of future work will be discussed, respectively.

5.2 CONCLUSION

Assessment on effect of geometry defect for steel pipe is studied in this project. The first objective for this research is to study about the effect geometry on steel pipeline with variable defect depth. The second objective is to analyses the effect of maximum pressure on different defect of geometry. The groove defect and rectangular defect shape are analyzed.

As the result showed in chapter 4, the geometry defect remarkably affect the stress strain distribution on the pipe. Corrosion defects (20%, 50% and 75% in depth) were evaluated using stress based criterion. Besides, geometry and depth defect influence the prediction of the burst pressure of pipelines. The presences of defect in pipeline surface will show the von Mises stress distribution at the defect base where it affected burst pressure. The deep defects are easy to fail compared with moderate defect and shallow defect.

The von Mises stress is higher at inner surface of the pipe compare to the outer pipe. However, width of defect does not affect much on the burst pressure of pipelines.

As a conclusion for overall data in chapter 4, the geometry defect and depth defect does have affect to the burst pressure. However, the width defect sizes do not influence the burst pressure of pipeline. Based on result been discuss at chapter 4, the ultimate tensile strength for groove defect achieved early burst pressure compared to the rectangular defect, but there are small different for the groove and rectangular defect to failed. Moreover, the burst pressure for width defect subjected to groove and rectangular defect are almost the same. It can be considered that, the width for groove and rectangular does not influence much the burst pressure of the pipeline rather than the depth of defect. The three industry codes (ASME B31G, Modified ASME and DNV-RP-F101) and FEA model in this research predict the burst pressure of pipe with corrosion defect is reduce as the depth of corrosion is increase. The prediction by FEA model shows the close result to DNV-RP-F101 code.

5.3 RECOMMENDATION

For the future work as to assessment on effect of geometry defect for steel pipe, the following consideration should be taken into consideration. As for suggestion upon future work, the material for analyses process should be various in order to simulate the defect with different type of material such as X65, X70 and so on. Furthermore, the experimental process should be performing as to compare the experimental value with the simulation result in order to get more precise result.

REFERENCES

Amirat, A., Mohamed-Chateauneuf, A., & Chaoui, K. (2006). Reliability assessment of underground pipelines under the combined effect of active corrosion and residual stress. *Pressure Vessels and Piping*, 107-117.

A.Cosham, P.Hopkins, & Macdonald, K. A. (2007). Best Practice for the assessment of defect in pipelines-Corrosion. *Engineering Failure Analysis*, 1245-1265.

Bedairi, B.,Cronin, D.,Hosseini, A., & Plumtree, A. (2012). Failure prediction for Crack-in-Corrosion defects in natural gas transmission pipelines. *Pressure Vessels and Piping*, 90-99.

Chiodo, M. S. G., & Ruggieri, C. (2009). Failure assessments of corroded pipelines with axial defects using stress-based criteria: Numerical studies and verification analyses. *Pressure Vessels and Piping*, 164-176.

Cosham, A., & Hopkins, P. (2004). The effect of dents in pipelines-guidance in the pipeline defect assessment manual. *Pressure Vessels and Piping*, 127-139.

Cheng, Y. F. (2007). Analysis of electrochemical hydrogen permeation through X-65 pipeline steel and its implications on pipeline stress corrosion cracking. *Hydrogen Energy*, 1269 – 1276.

Domizzi, G., Anteri, G., & Ovejero-Garcia, J. (2001). Influence of sulphur content and inclusion distribution on the hydrogen induced blister cracking in pressure vessel and pipeline steels. *Corrosion Science,* 325-339.

H.Adib, Jallouf, S., C.Schmitt, A.Carmasol, & G.Pluvinage. (2007). Evaluation of the effect of corrosion defects on the structural integrity of X52 gas pipelines using the SINTAP procedure and notch theory. *Pressure Vessels and Piping*, 123-131.

H.Adib-Ramezani, Jeong, J., & G.Pluvinage. (2006). Structural integrity evaluation of X52 gas pipes subjected to external corrosion defects using the SINTAP procedure. *Pressure Vessels and Piping*, 420-432.

Jr., D. B. N., , R. R. M., Jacob, B. P., & Souza, E. d. (2010). Procedures for the strain based assessment of pipeline dents. *Pressure Vessels and Piping*, 254-265.

Li, S.-X., Yu, S.-R., Li, H.-L., & Liang, R. (2009). Predicting corrosion remaining life of underground pipelines with a mechanically-based probabilistic model *Petroleum Science and Engineering*, 162-166.

L.Y.Xu, & Y.F.Cheng. (2012). Reliability and failure pressure prediction of various grades of pipeline steel in the presence of corrosion defects and pre-strain. *Pressure Vessels and Piping*, 75-84.

Ma, B., Shuai, J., Liu, D., & Xu, K. (2013). Assessment on Failure Pressure of High strength pipeline with corrosion defects. *Engineering Failure Analysis*.

Macdonald, K.A., & Cosham, A. (2005). Best practice for the assessment of defects in pipelines – gouges and dents. *Engineering Failure Analysis*, 720-745.

Macdonald, K. A., Cosham, A., Alexanderc, C. R., & Hopkinsd, P. (2007). Assessing mechanical damage in offshore pipelines – Two case studies. *Engineering Failure Analysis*,1667–1679.

Meresht, E. S., Farahani, T. S., & Neshati, J. (2011). Failure analysis of stress corrosion cracking occurred in a gas transmission steel pipeline. *Engineering Failure Analysis*, 963–970.

Netto, T. A., Ferraz, U. S., & Estefen, S. F. (2005). The effect of corrosion defects on the burst pressure of pipelines. *Constructional Steel* 1185-1204.

Sojka, J., Jérôme, M., Sozańska, M., Váňová, P., Rytířová, L., & Jonšta, P. (2008). Role of microstructure and testing conditions in sulphide stress cracking of X52 and X60 API steels *Materials Science and Engineering*, 237-243.

Shoji, T., Lu, Z., & Murakami, H. (2010). Formulating stress corrosion cracking growth rates by combination of crack tip mechanics and crack tip oxidation kinetics *Corrosion Science*, 769-779.

Teixeira, A. P., Soares, C. G., Netto, T. A., & S.F.Estefen. (2008). Reliability of pipelines with corrosion defects. *Pressure Vessels and Piping*, 228-237.

Tanguy, B., Luu, T. T., Perrin, G., Pineau, A., & Besson, J. (2008). Plastic and damage behaviour of a high strength X100 pipeline steel: Experiments and modelling. *Pressure Vessels and Piping*, 322-335.

Venegas, V., Caleyo, F., Baudin, T., Espina-Hernández, J. H., & Hallen, J. M. (2011). On the role of crystallographic texture in mitigating hydrogen-induced cracking in pipeline steels. *Corrosion Science*, 4204–4212.

W. Zhou, and G.X. Huang, 'Model Error Assessments of Burst Capacity Models for Corroded Pipelines', *International Journal of Pressure Vessels and Piping* (2012), 99-10.

APPENDIX A

GANTT CHART: FINAL YEAR PROJECT 1

GANTT CHART: FINAL YEAR PROJECT 1

	Task Name		1	2	3	4	5	6	7	8	9	10	11	12	13	14
1	FYP Title	P														
		A														
	Research on FYP title															
2	Review Research Title	P														
		A														
3	Find Literature Review	P														
		A														
4	Plan Work Schedule	P														
		A														
5	Learn MSC Software	P														
		A														
6	Prepare Introduction	P														
		A														
7	Determine Methodology	P														
		A														
8	Write Abstract	P														
		A														
9	Compile Proposal	P														
		A														
10	Finalize Proposal	P														
		A														
11	Submit Proposal	P														
		A														

P = Plan

A = Actual

GANTT CHART: FINAL YEAR PROJECT 2

	Week															
Task	**1**	**2**	**3**	**4**	**5**	**6**	**7**	**8**	**9**	**10**	**11**	**12**	**13**	**14**	**15**	**16**
Case 1																
Case 2																
Case 3																
Case 4																
Case 5																
Case 6																
Case 7																
Case 8																
Case 9																
Case 10																
Case 11																
Case 12																
Case 13																
Case 14																
Case 15																
Case 16																
Case 17																
Case 18																
Tabulated result																
Analysis the result																
Final Year Project Presentation																
Writing analysis report																

APPENDIX B

SPECTRO ANALYSIS RESULT FOR MATERIAL GRADE B

FOUNDRY LABORATORY
FACULTY OF MECHANICAL ENGINEERING
UNIVERSITI MALAYSIA PAHANG

Chemical Results

Date: 11/03/2012

Sample ID

Material: steel pipe

Customer: Ali

Dimension

Commission

Filter metal

Lab-no:

Heat treatment

Reference no:

Heat-no

Spectrometer Foundry-MASTER Grade

	Fe	C	Si	Mn	P	S	Cr	Mo
1	98,5	0,267	0,354	0,564	< 0,0100	< 0,0100	0,0285	< 0,0100
2	98,8	0,249	0,288	0,552	< 0,0100	< 0,0100	0,0247	< 0,0100
3	98,8	0,257	0,286	0,562	< 0,0100	< 0,0100	0,0264	< 0,0100
Ave	98,7	0,258	0,309	0,559	< 0,0100	< 0,0100	0,0265	< 0,0100

	Ni	Al	Co	Cu	Nb	Ti	V	W
1	0,0174	0,0499	< 0,0100	< 0,0050	< 0,0050	0,0097	< 0,0050	< 0,0250
2	0,0117	0,0138	< 0,0100	< 0,0050	< 0,0050	0,0042	< 0,0050	< 0,0250
3	0,0132	0,0255	< 0,0100	< 0,0050	< 0,0050	0,0041	< 0,0050	< 0,0250
Ave	0,0141	0,0298	< 0,0100	< 0,0050	< 0,0050	0,0060	< 0,0050	< 0,0250

	Pb
1	< 0,0500
2	< 0,0500
3	< 0,0500
Ave	< 0,0500

Foundry Laboratory
Faculty of Mechanical Engineering
Universiti Malaysia Pahang
26600 Pekan, Pahang, MALAYSIA
Tel: +6094242213 / 2270 / 2217
Fax: +6094242202
Website: http://fkm.ump.edu.my

Test by: Verify by

APPENDIX C

VON MISES STRESS AND PRESSURE APPLIED ON PIPE

GROOVE DEFECT DATA

Case 1: Pressure applied = 160MPa.

20% depth defect, d_g = 0.2mm

XYDATA,	
0	0
2	45.97186
4	91.91772
6	137.8423
8	183.7456
9	229.6508
10	275.5156
11	321.3597
12	367.1831
13	367.5614
14	356.3007
15	345.3471
16	338.6263
17	339.9637
18	341.6551
19	343.1849
20	345.2431
21	347.7465
22	350.4688
23	353.6252
24	357.041
25	360.4095
26	363.9966
27	366.1954
28	368.3087
29	370.5179
30	372.9833
31	375.9315
32	379.0232
33	382.302
34	385.2483
35	387.8849
36	390.7166
37	393.8574
38	397.4282
39	401.3138
40	405.7616
41	410.9758
42	416.7388
43	422.9051
44	428.9323
45	435.7902
46	443.1512
47	451.5835
48	460.2952
49	470.068
50	480.5008
51	491.6551
52	503.3005
53	515.606
55	533.8588

Case 2: Pressure applied = 160MPa.

20% depth defect, d_g = 0.5mm

XYDATA,	
0	0
2	8.943294
4	17.88366
6	26.82178
8	35.75765
9	44.69464
10	53.62661
11	62.55641
12	71.48406
13	80.40953
14	89.33288
15	98.25407
16	106.8466
17	115.2085
18	123.4053
19	131.075
20	138.398
21	145.2501
22	151.9221
23	157.9838
24	163.3952
25	168.5715
26	173.1237
27	177.2009
28	181.0192
29	184.391

30	187.5297
31	190.3792
32	193.0938
33	195.6688
34	198.1758
35	200.5875
36	202.9094
37	205.1597
38	207.5727
39	210.1008
40	213.1023
41	216.5715
42	220.7234
43	226.4311
44	234.1536
45	244.7557
46	258.5993
47	278.5887
48	305.3978
49	343.8615
50	394.2636
51	461.2668
52	493.7004
53	505.5147
55	525.1565

Case 3: Pressure applied = 160MPa.

20% depth defect, d_g = 1 mm

XYDATA,	
0	0
2	7.311669
4	14.62019
6	21.92609
8	29.22939
9	36.5322
10	43.83055
11	51.12634
12	58.41956
13	65.71022
14	72.99834
15	80.28392
16	87.56697
17	94.78299
18	101.7582
19	108.5677
20	115.1734
21	121.4589
22	127.5134
23	133.2301
24	138.6861
25	143.7555
26	148.4954
27	152.8543
28	156.8454
29	160.4576
30	163.759
31	166.7528
32	169.5226
33	172.1087
34	174.5543
35	176.9028
36	179.2047
37	181.5541
38	184.0411
39	186.6668
40	189.4542
41	192.615
42	196.4779
43	201.4942
44	208.6544
45	218.6135
46	232.7163
47	253.254
48	297.0416
50	390.1995
52	484.039
54	545.1161
56	555.6408
59	568.1693
62	581.7763

Case 4: Pressure applied = 100MPa.

50% depth defect, d_g = 0.2 mm

XYDATA,	
0	0
2	67.29978
4	134.5365
6	201.7213
8	268.8543
9	335.994
10	402.3835
11	387.5187
12	373.7149
13	360.2624
14	348.952
15	350.5759
16	354.3458
17	359.6399
18	365.2083
20	368.7823
21	371.5443
22	374.9929
23	378.9843
24	383.4782
25	387.6728
26	391.7747
27	396.3769
28	401.2329

30	406.4394
31	412.7319
32	419.6545
34	427.0208
35	434.0876
36	441.6344
38	449.0844
39	456.6252
40	463.7991
42	471.3719
43	478.5655
44	486.1121
45	493.8257
46	501.3286
47	508.9279
48	516.2488
49	523.5512
50	530.7578
51	537.9423
52	544.7927
53	551.3846
54	557.5469
55	563.7661
56	570.0171
57	575.989
58	581.1323
60	584.7189

Case 5: Pressure applied = 100MPa.

50% depth defect, d_g = 0.5 mm

XYDATA,	
0	0
2	15.39397
4	30.77462
6	46.14433
8	61.50316
9	76.86197
10	92.20078
11	107.5289
12	121.4959
13	134.5717
14	145.4116
15	155.5843
16	164.0537
17	171.9588
18	179.4093
19	186.3119
20	192.7365
21	198.3555
22	202.3571
23	205.5726
24	208.261
25	210.6134
26	212.7645
27	214.6497
28	216.9118
29	219.2553

30	223.5144
31	232.7928
32	242.9682
33	254.9741
35	269.6222
37	285.5832
39	297.9458
41	309.0383
43	324.1594
44	341.1589
46	360.2974
47	382.809
48	411.7482
49	444.824
50	475.336
51	489.1455
52	501.6877
53	512.3361
54	521.1633
55	529.1276
56	537.1544
57	545.9646
58	554.0408
59	564.3882
60	576.563

Case 6: Pressure applied = 100MPa.

50% depth defect, d_g = 1 mm

XYDATA,	
0	0
2	38.23438
4	76.42971
6	114.5927
8	152.7237
9	190.8457
10	228.9145
11	266.9514
12	304.9564
13	342.9296
14	342.4553
15	333.8829
16	334.7524
17	335.2431
18	335.9551
19	337.0423
20	338.5028
21	340.3028
22	342.335
23	344.6353
24	347.1265
25	349.8637
26	352.8008
27	356.0435
28	359.4631
29	361.894
30	364.1425
31	366.8376
32	369.7446
33	372.9195
34	376.3382
35	380.0043
36	382.8625
37	386.1733
38	389.827
39	393.7666
40	398.047
41	402.9756
42	408.557
43	414.2015
44	419.8842
45	425.4297
46	431.3428
47	436.951
48	442.7355
49	448.6326
50	454.1877
51	460.3628
52	466.7033
53	474.2007
55	482.8373

Case 7: Pressure applied = 60MPa.

75% depth defect, d_g = 0.2 mm

XYDATA,	
0	0
2	86.10616
4	172.0923
6	257.9785
8	343.7656
9	384.1107
11	366.2472
12	349.4959
13	346.2684
14	350.2104
15	354.7877
16	359.648
17	365.5931
18	369.4632
19	373.8262
20	378.5385
21	383.8037
22	388.7042
24	393.6412
25	398.822
26	404.1351
28	411.07
30	418.0485
31	425.3636
32	432.4586
34	439.5977
35	446.0199
36	452.7266
37	459.1768
38	465.7573
39	471.9912
40	478.2051
41	484.3547
42	490.5324
43	496.4161
44	502.3599
45	507.9518
46	513.4948
47	518.93
48	524.33
49	529.974
51	536.4174
53	543.7139
55	551.6609
56	560.4078
57	569.8284
58	577.7461
59	582.5671
61	588.2435
63	592.9183
65	589.9717

Case 8: Pressure applied = 60MPa.

75% depth defect, d_g = 0.5 mm

XYDATA,	
0	0
2	28.41726
4	56.79472
6	85.13861
8	113.4491
9	141.7512
10	169.9982
11	191.5452
12	208.96
13	223.2666
14	234.003
15	243.0142
16	251.6928
17	259.5074
18	256.5407
19	253.8723
20	252.4331
21	251.5946
22	251.0057
23	250.9847
24	251.4562
25	252.1244
26	253.1644
27	254.4864
28	255.9499
29	258.0938

30	260.9283
31	264.7493
32	269.4532
33	275.3908
34	283.6904
35	293.3677
36	305.3828
37	318.0694
38	331.622
39	350.0309
40	372.9576
41	397.0162
42	423.8654
43	453.1461
44	486.6206
45	510.5044
47	523.9507
49	534.7447
51	547.6213
52	558.3704
53	569.6812
55	578.2581
57	588.7327
59	598.6428
61	607.5201

Case 9: Pressure applied = 60MPa.

75% depth defect, d_g = 1 mm

XYDATA,	
0	0
2	47.67575
4	95.28206
6	142.8304
8	190.3213
9	237.7932
10	285.1722
11	332.4941
12	345.8147
13	335.8829
14	336.7886
15	337.4219
16	338.2701
17	339.6831
18	341.6341
19	344.0073
20	346.7121
21	349.6583
22	352.8663
23	356.2658
24	359.8898
25	362.4827
26	364.8006
27	367.5728
28	370.4923
29	373.5966
30	376.8347
31	380.2733
32	383.0044
33	385.8498
34	388.9338
35	392.122
36	395.4948
37	398.9413
38	402.8674
39	407.279
40	411.7067
41	416.3007
42	420.7555
43	425.1356
44	430.1322
45	436.4206
47	444.2772
49	453.7779
50	464.4214
51	476.2885
53	489.0054
55	502.7493
57	516.5897
59	530.2175
61	542.6843

RECTANGULAR DEFECT

Case 1: Pressure applied = 180MPa.

20% depth defect, w_c = 0.2 mm

XYDATA,	stress
0	0
2	34.01268
4	68.00733
6	101.9874
8	135.9529
9	169.9227
10	203.8628
11	237.7887
12	271.7007
13	305.5986
14	339.4826
15	351.7769
16	351.15
17	350.4863
18	341.8303
19	337.9893
20	337.6174
21	339.4126
22	341.4553
23	343.7763
24	346.2897
25	348.791
26	351.5098
27	354.0061
28	356.2667
29	358.7452
30	361.2991
31	364.083
32	367.0517
33	370.2237
34	373.5779
35	376.5728
36	379.8111
37	383.4165
38	387.4969
39	392.6945
40	398.9568
41	405.5643
42	413.0903
43	421.8418
44	432.3205
45	444.0625
46	456.4085
47	469.871
48	489.1909
50	511.1698
52	532.3418
54	551.6552
56	565.207
59	575.5733
63	578.5693

Case 2: Pressure applied = 200MPa.

20% depth defect, w_c = 0.5 mm

XYDATA,	stress
0	0
2	28.33244
4	56.6475
6	84.94836
8	113.2351
9	141.523
10	169.7841
11	198.0314
12	226.2649
13	254.4847
14	282.6909
15	313.7294
16	320.8439
17	322.1421
18	323.9316
19	327.8898
20	334.177
21	336.1923
22	337.8378
23	338.9783
24	340.3083
25	341.8195
26	343.6949
27	345.9418
28	348.2989
29	351.0223

30	353.9407
31	356.2197
32	358.6557
33	361.3213
34	364.3685
35	367.5633
36	371.114
37	375.3875
38	379.4092
39	384.6226
40	391.7298
41	401.0311
42	410.252
43	421.8983
45	440.7891
47	463.0141
49	485.8984
51	508.6826
53	530.6855
56	548.542
59	563.3245
63	573.1464
68	578.8718
74	584.1229
80	589.8519

Case 3: Pressure applied = 200MPa.

20% depth defect, w_c = 1 mm

XYDATA,	stress
0	0
2	22.35557
4	44.69666
6	67.02585
8	89.34322
9	111.6602
10	133.9557
11	156.2396
12	178.5119
13	200.7727
14	223.0221
15	245.2599
16	267.4864
17	292.0293
18	305.0786
19	307.5497
20	311.0864
21	316.3212
22	323.1262
23	330.6007
24	336.8818
25	336.946
26	337.9531
27	339.2377
28	340.4937
29	341.9948
30	343.7589
31	345.7828
32	348.0994
33	350.7652
34	353.8665
35	357.051
36	359.8191
37	363.0128
38	366.4615
39	371.0306
40	376.4033
41	381.5395
42	387.659
43	397.743
45	413.1874
47	431.4946
49	452.229
51	473.8534
53	494.966
55	515.2211
58	533.7543
61	547.7854
64	559.8668
68	569.6825
72	574.0838

Case 4: Pressure applied = 100MPa.

50% depth defect, w_c = 0.2 mm

XYDATA,	stress
0	0
2	46.09689
4	92.15361
6	138.1774
8	184.1683
9	230.1646
10	276.0971
11	321.9976
12	370.3984
13	372.102
14	365.9827
16	354.2396
17	345.8188
18	343.709
19	346.4309
20	349.9007
21	353.2698
22	356.1259
23	359.3905
24	363.1378
25	367.0009
26	371.0034
27	374.8802
28	378.6508
29	382.3944

30	386.6971
31	391.767
32	397.3043
33	403.2391
34	408.6351
35	414.6938
36	421.0209
37	427.4849
38	434.5109
39	442.2112
40	449.8513
41	457.308
42	465.0209
43	472.7399
44	480.5406
45	488.1325
46	495.6611
47	502.8986
48	510.1433
49	517.1321
50	523.8395
51	530.2803
52	536.6123
53	543.5834
54	551.0935
56	558.6226

Case 5: Pressure applied = 100MPa.

50% depth defect, w_c = 0.5 mm

XYDATA,	STRESS
0	0
2	37.61584
4	75.19653
6	112.7482
8	150.2711
9	187.7937
10	225.2635
11	262.705
12	300.1182
13	340.0208
14	347.4339
15	348.4069
16	349.5024
17	344.4808
18	342.6699
19	343.4178
20	346.0717
21	348.5809
22	351.4004
23	353.645
24	356.0317
25	358.9221
26	361.7251
27	364.9189
28	368.4279
29	371.7776

30	375.1571
31	378.8953
32	382.737
34	386.7451
36	391.3162
38	396.2084
39	401.34
40	406.5736
41	412.0677
42	417.1553
43	422.6138
45	428.2235
46	433.9186
47	439.5687
48	445.776
49	451.9067
50	458.2208
51	464.0466
52	469.9265
53	475.8648
54	481.5888
55	487.7569
56	494.9153
58	503.2706
60	511.8933

Case 6: Pressure applied = 110MPa.

50% depth defect, w_c = 1 mm

XYDATA,	stress
0	0
2	34.90707
4	69.77518
6	104.611
8	139.4147
9	174.2148
10	208.9584
11	243.6704
12	278.351
13	313.0617
14	332.6043
15	334.2174
16	335.9829
17	340.122
18	340.2438
19	340.0094
20	342.5558
21	345.3826
22	347.4615
23	350.0958
24	352.6134
25	354.5513
26	356.8015
27	359.4175
28	362.2843
29	365.5896
30	369.144
31	372.4693
32	376.194
33	379.8914
34	383.5944
35	387.5764
37	392.1802
38	396.9917
39	402.0552
40	407.0617
41	412.0291
42	416.7935
43	421.5595
44	426.5822
45	431.3838
46	436.4584
47	442.0112
48	448.332
50	456.1592
52	465.1993
54	474.9443
56	485.1163
58	495.448
60	506.2813
62	517.5277

Case 7: Pressure applied = 60MPa.

75% depth defect, w_c = 0.2 mm

XYDATA,	stress
0	0
2	62.32767
4	124.5741
6	186.7531
8	248.865
9	310.9747
10	344.1545
11	343.8041
12	340.9833
13	338.1861
14	341.0267
16	344.6756
18	348.053
19	352.1936
20	355.8017
21	359.4661
22	363.3376
23	367.718
24	371.9058
25	376.3023
26	380.0778
27	384.0058
28	388.2791
29	393.1482

30	398.7148
31	403.783
32	408.7212
33	413.9167
34	419.0129
35	424.2511
36	429.3985
37	434.9866
38	440.6058
39	446.3903
40	451.896
41	457.5619
42	463.2411
43	468.9278
44	474.4558
45	480.0748
46	486.293
47	493.7077
48	502.1822
49	511.2989
51	521.0292
53	531.0369
55	541.9971
57	553.0071
59	561.6445
61	570.2474
64	577.8341

Case 8: Pressure applied = 60MPa.

75% depth defect, w_c = 0.5 mm

XYDATA,	stress
0	0
2	49.6125
4	99.15755
6	148.6464
8	198.0795
9	247.5048
10	296.8332
11	327.3487
12	330.1139
13	334.7293
14	339.1553
15	339.5078
16	342.3575
17	344.7278
18	347.4759
20	350.538
21	353.1727
22	355.7232
23	358.4232
24	361.3862
25	364.5943
26	368.1353
27	371.588
28	375.1395
29	378.1843

30	381.2726
31	384.4745
32	387.8208
33	391.5612
34	395.6528
35	399.9808
36	404.0895
37	407.8792
38	411.7272
39	415.6151
40	419.4413
41	423.3061
42	427.2786
43	431.4028
44	435.6602
45	440.4134
47	446.8152
49	454.3239
51	463.0838
53	473.5504
55	484.8289
57	497.1507
59	510.7011
61	523.6298
63	535.8712
65	547.5798

Case 9: Pressure applied = 60MPa.

75% depth defect, w_c = 1 mm

XYDATA,	
0	0
2	37.82407
4	75.59552
6	113.3231
8	151.007
9	188.6811
10	226.282
11	263.8398
12	302.8134
13	321.8889
14	325.1055
15	329.9146
16	339.1315
17	337.3573
18	339.2737
19	340.592
20	342.3543
21	344.1918
22	346.1127
23	348.0901
24	350.191
25	352.4137
26	354.4134
27	356.1198
28	357.9717
29	359.9454

30	362.0039
31	364.2001
32	366.5493
33	369.0833
34	371.573
35	373.897
36	375.9478
37	378.0285
38	380.304
39	382.6414
40	385.0113
41	387.5284
42	390.2296
43	392.8223
44	396.2795
46	402.2433
48	410.4944
50	420.3488
52	432.359
54	445.7905
55	459.7437
56	473.8735
58	487.7891
60	500.6317
62	512.8428